# "Design-analysis of Silicon based Photonic crystal waveguide for On-chip Slow Light Applications"

Dissertation submitted towards the partial fulfilment of requirement for the award of degree of

## Master of Engineering

## In

## Electronics and Communication Engineering


**Submitted by:**

Ankita Sharma

(801261004)

**Under the guidance of:**

Dr. Mukesh Kumar



**ELECTRONICS AND COMMUNICATION ENGINEERING DEPARTMENT**

**THAPAR UNIVERSITY**

**(Established under the section 3 of UGC Act, 1956)**

**PATIALA – 147004 (PUNJAB) July 2014**

# DECLARATION

I Ankita Sharma, hereby certify that the work which is being presented in dissertation entitled "Design-analysis of Silicon based Photonic crystal waveguide for On-chip Slow Light Applications" is an authentic record of my study carried out as requirement for the award of degree of ME (Electronics and Communication Engineering) at Thapar University, Patiala, under the supervision of "Dr. Mukesh Kumar".

The matter presented in this dissertation has not been submitted in any other university/institute for the award of any other degree.

Date: 1/7/14

"Ankita Sharma"

(801261004)

It is certified that the above statement made by the student is correct to the best of my knowledge and belief.

Date: 1/7/14

"Dr. Mukesh Kumar"

Assistant Professor

ECED

Countersigned by:

1/7/2014

"Dr. Sanjay Sharma"

Professor and Head ECED
Thapar University, Patiala

"Dr. S.K. Mohapatra"

Dean of Academic Affairs
Thapar University, Patiala

# TABLE OF CONTENTS

# ACKNOWLEDGEMENT

I would like to express my special thanks and deep sense gratitude to my dissertation Advisor, Dr. Mukesh Kumar, Assistant Professor, Electronics & Communication Engineering Department, Thapar University, Patiala for their continuous indefatigable guidance, which paved me on to the path to carry this dissertation. He has always been very encouraging and offered invaluable advice. I am highly indebted to them for their efforts and invaluable suggestions during the period of work.

I am also thankful to Dr. Sanjay Sharma, Professor and Head, Dr. Kulbir Singh, Associate Professor, Electronics & Communication Engineering Department, Thapar University, Patiala for their valuable advice and helped in all possible ways for the completion of my dissertation work.

I wish to express thanks to all those persons who with their encouraging words and suggestions have contributed directly or indirectly for the completion of this work.

# ABSTRACT

Line-defect photonic crystal waveguides which is different from conventional dielectric waveguides such as optical fiber are receiving considerable attention. Our proposed waveguide structure is based on silicon photonics. Different optical components can be connected with each other using proposed silicon waveguide to establish very fast communication between circuit boards, between chips on a board, or even within single chips.

A low-loss and flat dispersion line-defect photonic crystal waveguide is proposed based on triangular lattice of two dimensional photonic crystals. Our main aim was to achieve flat band slow light in silicon in a photonic crystal waveguide with large delay bandwidth product and low GVD by shifting the positions of rows which are adjacent to the waveguiding region. We propose two design approaches to design flat dispersion line defect waveguide with low loss. In first set of approach, lattice constant value remains constant throughout all proposed structures and in second set of approach, it is varied. A delay-bandwidth product (NDBP) with acceptably small group velocity dispersion in photonic crystal waveguide is achieved. We proposed three structures by shifting the first two rows of holes adjacent to the waveguide. Larger group index values of 36.16, 44.9 and 53.95 over flat bandwidth of 15.7, 13.66 and 9.9 nm along with NDBP values of 0.351, 0.38 and 0.329 are obtained. NDBP value is further improved by taking different lattice constant values for all three structures and higher group indices 36.60, 46.52 and 54.58 over flat bandwidth of 18.82, 14.05 and 11.19 nm are reported. GVD parameter is also found to be low for all the structures. The reported results can be useful in realizing flat band slow light in silicon with improved waveguiding characteristics. To further test the practical applicability of our waveguide the buffering capacity is calculated which is found to be as high as 140 bits. Both the approaches are better from fabrication point of view as controlling the radius of holes at nano-metre scale brings fabrication challenges. Generation of slow light is a promising solution for buffering and time-domain processing of optical signals and also offers the possibility for spatial compression of optical energy and the enhancement of linear and nonlinear optical effects.

# LIST OF FIGURE

# LIST OF TABLE

# CHAPTER 1

# Introduction to Photonic Crystals

## 1.1 Motivation

In the last few decades, a new frontier has opened up due to tremendous advancement of semiconductor technology which have brought incredible changes to our society and the life of people. The aim has become to control the optical properties of materials. A massive range of technological developments become possible by engineering of such materials that respond to light waves over a desired range of frequencies. They can perfectly reflect the light waves, or allow them to propagate only in certain directions, or can also confine them within a specified volume [1]. The introduction of components such as optical fibers or integrated ridge waveguides which were based on principle of total internal reflection for light guidance has bought revolutionary changes in the telecommunication and optical industry. Apart from that, another way of controlling light based on Bragg diffraction has already been used in many devices like dielectric mirrors. The principle of dielectric mirrors based on one-dimensional (1D) light reflection was generalized to two and three dimensions in 1987 [2, 3] which leaded to a new class of materials: photonic crystals. Photonic crystals are formed by periodic arrangement of dielectric constants or index of refraction. They are called crystals because of their periodicity and photonic because they interact with light.

During the 21st century, there is a vision that photonic devices may take over the task of electronic devices. Through the use of amazingly analogous theoretical and fabrication approaches, photonic crystals assure to give us control over the flow of photons, and with their capability to interact with light on a wavelength scale they have the potential to provide the means for photonic integration. By properly designing photonic crystals as main components for devices optical properties of materials could be controlled which could be used in extracting light to useful radiation, in efficiency boosting ,in improving brightness of LEDs, in all-optical switching ,preventing photon emission into certain optical modes for low threshold micro cavity lasers, and wave guiding beyond the limits of total internal reflection for highly compact systems containing tight bends, for light

signal transfer, splitters etc. Realization of these devices require the need to understand the fundamental properties of photonic crystals with their limiting factors such as propagation losses and capability to be fabricated with today's technology [1].

With time optical communication has become potential area of research due to certain reasons:

1. Optical communication links possesses larger bandwidth than copper or microwave links; hence enhancing information capacity on a given link.

2. Attenuation in glass fibers is less than experienced in microwave systems or copper. Thus less number of repeaters is required, which enabled longer distance communication with low cost.

3. Due to smaller size and light in weight they are preferably employed in crowded ducts or aircraft.

4. Optical waveguides are tricky to tap or scrutinize, so data security is higher.

5. Optical waveguides are resistant from induced cross talk, ground loops, electromagnetic interference etc.

6. Semiconductor technology has developed a family of lasers, detectors, and other integrated optical devices that are well-suited with optical fibers in power, wavelength, and size.

## 1.2 Photonic Crystals- Introduction

### 1.2.1 Photonic Crystals- Basics

Although photonic crystals have been studied in one form or another since 1887, the term "photonic crystal" was first used by Eli Yablonovitch and Sajeev John in their papers on photonic crystals in 1987. Yablonovitch's main motivation was to engineer the photonic density of state to control the spontaneous emission of materials embedded within the photonic crystal; John's methodology was to use photonic crystals to affect the localization and control of light. Their work addressed the engineering of a structured material which exhibits range of frequencies termed as bandgap at which the propagation of electromagnetic waves is not allowed [2, 3]. The electron spectrum found from purely periodic ionic lattice is not exact. There were many body effects in the solid like the thermal motion of the atoms, presence of defects and impurities. And these results leaded

to the strong determination of the true spectrum which was a tricky problem. The Maxwell equations are basically used to govern the scattering of light. Thus the problem was resolved easily and people achieved high accuracy in designing of materials. Thermal expansion of the materials is generally controllable and leads to a small swing of the operating wavelength (about a few nm for particular electronic devices under particular operating environment the temperature deviates), which is limited by the Thermal effects only. However, the troubles of thermal scattering and many body effects are normally not present in photonic crystal. Research related to photonic crystals began to rise exponentially after 1987. However, due to the complexity in optical scale fabrication of these structures, previous studies were either theoretical or in the microwave regime. Due to this photonic crystals can be built on far more readily accessible centimeter scale. By 1993, Yablonovitch had confirmed the first three-dimensional photonic band-gap in the microwave regime [4]. In 1996, Thomas Krauss made the first demonstration of a two-dimensional photonic crystal at optical wavelengths [5]. This opened up new area for photonic crystals fabrication by using the methods of semiconductor industry. At present photonic crystal slabs are used which are nothing but two dimensional photonic crystals "etched" into slabs of semiconductor. Research is in progress around the world to utilize photonic crystal slabs in integrated computer chips, in order to advance the optical processing of communications both on-chip and between chips.

### 1.2.2 Photonic Crystals Applications

Photonic crystals without a complete Photonic Band Gap can be designed to obtain super collimators and super-lenses [6] (Fig. 1.1) Based on the same effect, two photons that impinge a photonic crystal with the same angle but a slightly dissimilar energy, may find Equi-frequency surfaces(EFS) with a very different curvature. As a result their propagation angles would be very different. This is known as super-prism effect. Fabrication of integrated circuits in which information carriers were photons instead of electrons is one of the most anticipated applications for photonic crystals. In this intellect wave-guides (WG) based on 2D photonic crystals have been designed (Fig. 1.2) and are being continuously improved by engineers [7]. Although there is already a large amount of work done on WGs based on total internal reflection, photonic crystals ensures lot of advantages. For example sharp bends in a photonic crystal based WG do not present losses as high as those based on total internal reflection.

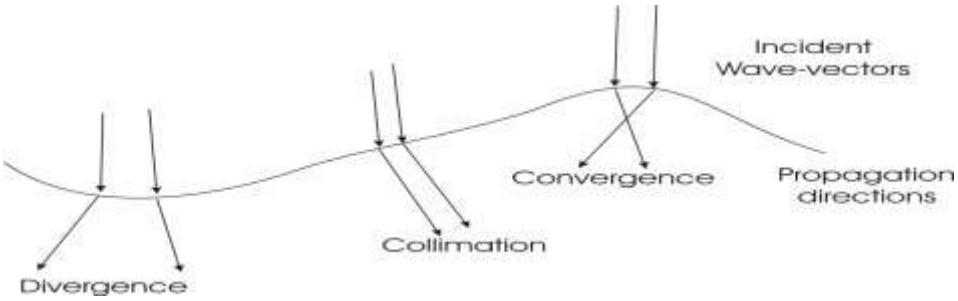


Figure 1.1: Behaviour of photons of same frequency for different curvatures of the EFS. For some range of directions and energies, photonic crystals can work as collimators, concave or convex lens [7].

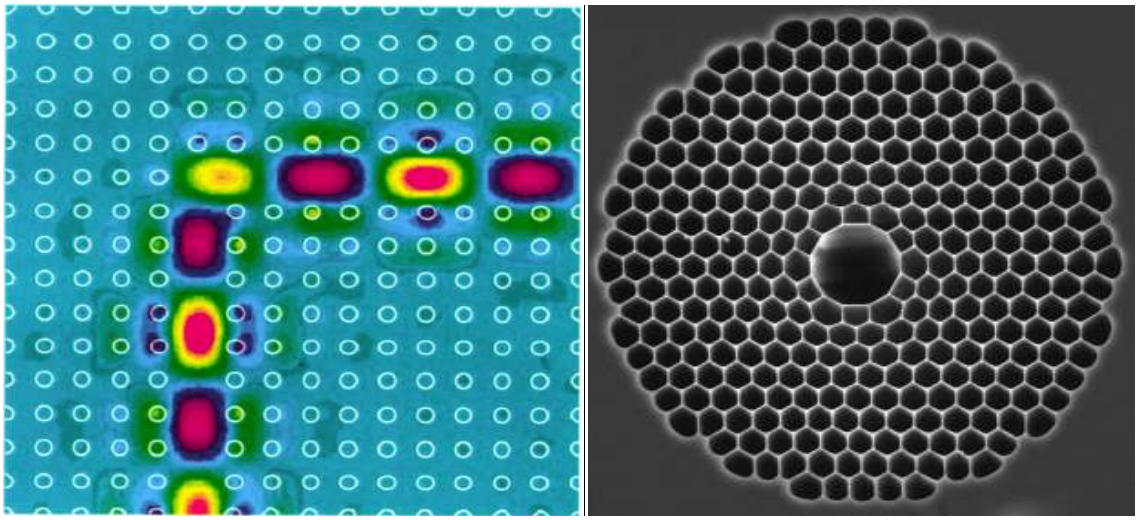

Figure 1.2: A two dimensional integrated photonic crystal circuit and hollow core photonic crystal fiber respectively [8, 9].

Broadly, Photonic crystal applications could be categorized in three areas Bandgap, Band edge and Band engineering. Bandgap engineering focuses on introducing defects in photonic crystal structure based on application, such as Photonic crystal slab with infinite height (2D) [8] and finite height (3D) has recently become popular due to variety of applications related to it [10, 11]. Micro cavity with high quality ($Q$) factor was another possible application of photonic crystal slab. Mainly laser generation desire this type of high $Q$cavity [8]. The density of states per unit volume for free photon is proportional to

$$\frac{1}{w\lambda^3} \tag{1.1}$$

The density of state reduces to zero if the frequency of operation lies within the bandgap of photonic crystal. The density of states per unit volume for the resonant frequency is proportional to

$$\frac{1}{\Delta w \Omega} \tag{1.2}$$

Where, $\Delta w$ represent the frequency width of the resonance and $\Omega$ represent the effective spatial volume. The improvement factor is given by

$$\frac{w}{\Delta w}\frac{\lambda^3}{\Omega} = \frac{Q}{\Omega/\lambda^3} \tag{1.3}$$

Improvement Factor is nothing but the quality factor of the cavity. Significant improvement of spontaneous emission occurs which is due to small spatial volumes and high $Q$ factor. The biggest improvement available is almost $Q$ when the smallest volume $\Omega$ have an order of the $\lambda^3$. It is vital to fabricate cavities with spatial dimensions which are comparable to the wavelength of light in order to achieve such largest improvement factors. Lithographic techniques are required for fabrication of cavities but for the realization of such nanocavities, point defect photonic crystals are one of the popular techniques. Apart from designing optical nanocavity, coupled resonator optical waveguides (CROWs) were considered as a new technique to direct light on a photonic chip [12] but they exhibited weak coupling between optical cavities and thus leaded to optical waveguide design through sequence of high- Q resonators which ensured perfect bend transmission [13]. Figure 1.3 shows laser structure based on band edge engineering. This laser consists of wafer A and B in which wafer A has active layer on which photonic crystal has been introduced. Together with both wafers photonic crystal is enclosed which constitutes the device. This device could operate as a surface-emitting device [14-16].

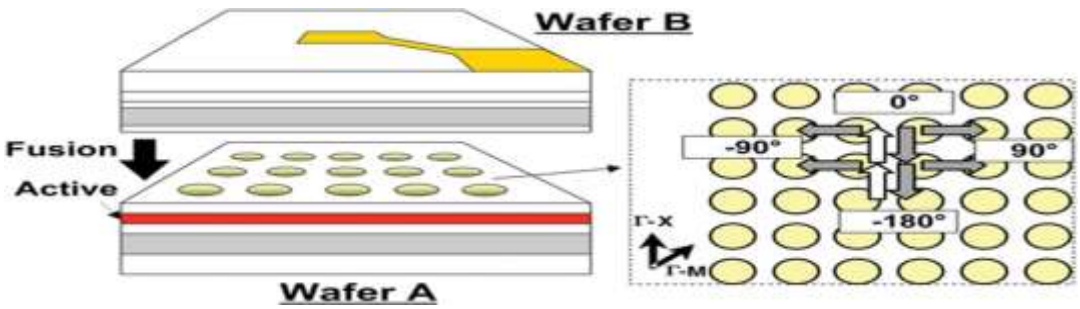


Figure 1.3 Laser structure constructed by band-edge engineering [17].

Band engineering focuses on the transmitted bands of photonic crystals. It utilizes the dispersion relations of these bands. Super prism phenomenon which was reported in 1998 uses these dispersion characteristics [16]. This phenomenon elaborates the effect of changes of wavelength and incident angle on characteristics of propagating light also negative refraction is observed if the refractive index contrast between high and low index of medium becomes large [18]. For controlling the propagation of optical pulses, such as velocity of pulsed light and for pulse shaping dispersion relations were utilized. Effects of low and high group velocity in line-defect waveguides in 2-D photonic crystal slabs also became research area of interest especially for delay lines and buffering applications. Light-emitting diodes based on photonic crystal but with improved light extraction efficiency also gained interests of researchers. Focus is mainly on applications for GaN system light-emitting diodes [19]. Nano processing and nano-imprinting based integration is also a very fascinating development area.

Photonic crystals remain desirable choice for operation and controlling the flow of electromagnetic waves amongst all optical materials. One dimensional photonic crystal are already in ample usage in the form of thin film optics applications ranging from low reflections to high reflection coatings on mirrors as well as on lenses to color changing paints and inks. For both conventional and proficient research the high dimensional photonic crystals are always of great attention and the two dimensional ones are being employed for commercial applications. Even today, three-dimensional photonic crystals are difficult to realize and thus they are still away from commercial applications. But they still exhibit considerable features such as optical nonlinearity which is necessary for the function of optical transistors and is used in optical computers, when manufacturability and principal difficulties such as technological aspects and other discontinuities remains under control. Numerous applications of photonic crystal will emerge as the study of photonic crystal steps forward. In this information age the variety of application of photonic crystal is simply limited by the edge of human minds.

## 1.3 Slow Light in Photonic Crystal Waveguide

In next generation information networks, path switching of optical packets at network nodes become vital and solutions that can perform the task with high data rate, low power consumption and high throughput are needed. All optical processing based photonic routers are being developed which avoids conversion to electrical domain and thus

reduces inefficiency introduced by optical-electronic conversion. Present solutions are based on mechanical delay lines and variable delay lines with optical switch but these are very slow. Slow light with low group velocity in Photonic crystal based waveguide has gained lot of attention as it is a potential applicant for buffering and time-domain processing of optical signals. It also exhibits the possibility for spatial compression of optical energy and the enhancement of linear and nonlinear optical effects. Photonic-crystal devices are outstanding choice for generating slow light, as they are well-suited with on-chip integration and room-temperature operation. They also exhibit wider bandwidth and zero or low dispersion propagation [20, 21].

## 1.4 Purpose and Outline of Work

The purpose of our research is to design and analyse photonic crystal waveguide for flat band slow light applications. In this dissertation, low dispersion flat band line-defect photonic crystal waveguide is proposed based on triangular lattice of two dimensional photonic crystals. Design and analysis of the slow light waveguide is performed with MIT Photonic Bandgap (MPB) package which is based on plane wave expansion method. In this dissertation we proposed two design approaches for the realization of efficient slow light characteristics, in both the approaches position of rows of holes adjacent to defect waveguide is shifted. In first approach, the lattice constant remains unchanged over all the designs and low dispersion and high group index bandwidth product for high group index values is obtained. In the second set of approach, the lattice constant is varied in all designs and improvised delay bandwidth product over larger bandwidth is obtained. To test the applicability of the proposed designs in buffering we calculated various parameters of buffering for the proposed PC waveguide.

Chapter 2 gives a theoretical introduction to the properties of photonic crystals starting with Maxwell's equations. These equations are cast as a linear Hermitian eigenvalue problem, a form in which many useful properties become apparent. The photonic crystal properties are then described by the characteristic photonic band structure or dispersion diagram representing the eigensolutions of the eigenvalue problem for a periodic dielectric structure.

Chapter 3 presents brief survey of published research on photonic crystal waveguide and slow light.

Chapter 4 discusses the design and results of line defect photonic crystal waveguide structure by shifting the position of rows of holes adjacent to defect waveguide. To test the applicability of the proposed designs we calculated various parameters such as buffering capacity of the proposed PC waveguide. Brief discussion is also made on suitability of proposed structures for buffering and delay based applications.

# CHAPTER 2

# Theory of Photonic Crystals

## 2.1 Wave Equations and Eigenvalue Problem

The optical properties of photonic crystals can be designed by basic idea about the interaction of light with periodic dielectric materials. For this basis, we must understand Maxwell equations, which elaborate the interaction of light with matter. We know that macroscopic electromagnetism which also includes the propagation of light in a photonic crystal is also governed by the four macroscopic Maxwell equations [1, 7].

$$\nabla . \mathbf{B} = 0$$
$$\nabla \times \mathbf{E} + \frac{\partial \boldsymbol{B}}{\partial t} = 0$$
$$\nabla \cdot \mathbf{D} = \rho$$
$$\nabla \times \mathbf{H} - \frac{\partial \boldsymbol{D}}{\partial t} = \mathbf{J} \qquad (2.1)$$

where (respectively) **E** and **H** are the macroscopic electric and magnetic fields, **D** and **B** are the displacement and magnetic induction fields, and **J** and ρ are the current and free charge densities. Propagation within a mixed dielectric medium consists of composite of regions of homogeneous dielectric material. It varies as a function of the (Cartesian) position vector **r** but the structure does not vary with time and also there are no free charges or currents. This composite need not be periodic. For such medium in which light propagates but there are no sources of light, we can set ρ = 0 and **J** = 0. Also we have,

$$\mathbf{D}(\mathbf{r}) = \varepsilon_0 \varepsilon(\mathbf{r})\, \mathbf{E}(\mathbf{r})$$

A similar equation relates:

$$\mathbf{B}(\mathbf{r}) = \mu_0 \mu(\mathbf{r})\, \mathbf{H}(\mathbf{r})$$

(where $\mu_0 = 4\pi \times 10{-}7$ Henry/m is the vacuum permeability), but for many dielectric materials the relative magnetic permeability μ(**r**) is very close to unity and we may set **B** = $\mu_0$**H** for simplicity. In that case, ε is the square of the refractive index n that may be

familiar from Snell's law and other formulas of classical optics. (In general, $n = \sqrt{\varepsilon\mu}$). With all of these assumptions in place, the Maxwell equations (1) become

$$\begin{aligned}
&\nabla \cdot \mathbf{H}(\mathbf{r}, t) = 0 \\
&\nabla \times \mathbf{E}(\mathbf{r}, t) + \mu_0 \frac{\partial \boldsymbol{H}(\boldsymbol{r},t)}{\partial t} = 0 \\
&\nabla \cdot [\varepsilon(\mathbf{r}).\mathbf{E}(\mathbf{r}, t)] = 0 \\
&\nabla \times \mathbf{H}(\mathbf{r}, t) - \varepsilon_0 \varepsilon(\mathbf{r}) \frac{\partial \boldsymbol{E}(\boldsymbol{r},t)}{\partial t} = 0
\end{aligned} \qquad (2.2)$$

In general, both **E** and **H** are complicated functions of both time and space. Because the Maxwell equations are linear, however, we can separate the time dependence from the spatial dependence by expanding the fields into a set of harmonic modes. This allows us to write a harmonic mode as a spatial pattern (or "mode profile") times a complex exponential:

$$\begin{aligned}
&\mathbf{H}(\mathbf{r}, t) = \mathbf{H}(\mathbf{r})\, e^{-i\omega t} \\
&\mathbf{E}(\mathbf{r}, t) = \mathbf{E}(\mathbf{r})\, e^{-i\omega t}
\end{aligned} \qquad (2.3)$$

To find the equations governing the mode profiles for a given frequency, we insert the above equations into (2.2). The two divergence equations give the conditions

$$\begin{aligned}
&\nabla \cdot \mathbf{H}(\mathbf{r}) = 0 \\
&\nabla \cdot [\varepsilon(\mathbf{r})\, \mathbf{E}(\mathbf{r})] = 0
\end{aligned} \qquad (2.4)$$

which have a simple physical interpretation: there are no point sources or sinks of displacement and magnetic fields in the medium. Equivalently, the field configurations are built up of electromagnetic waves that are transverse. Suppose if we have a plane wave $\mathbf{H}(\mathbf{r}) = \mathbf{a} \exp(i\mathbf{k} \cdot \mathbf{r})$ for some wave vector **k**, than equation (2.4) will require $\mathbf{a} \cdot \mathbf{k} = 0$. We can now focus our attention only on the other two of the Maxwell equations .The two curl equations relate $\mathbf{E}(\mathbf{r})$ to $\mathbf{H}(\mathbf{r})$:

$$\begin{aligned}
&\nabla \times \mathbf{E}(\mathbf{r}) - i\omega\mu_0 \mathbf{H}(\mathbf{r}) = 0 \\
&\nabla \times \mathbf{H}(\mathbf{r}) + i\omega\varepsilon_0 \varepsilon(\mathbf{r}) \mathbf{E}(\mathbf{r}) = 0
\end{aligned} \qquad (2.5)$$

These equations can be decoupled in the following way. We will Divide the bottom equation of (2.5) by ε(**r**), and then take its curl. We will use the first equation to eliminate **E**(**r**). The constants $\varepsilon_0$ and $\mu_0$ can be combined to yield the vacuum speed of light, $c = 1/\sqrt{\varepsilon_0\mu_0}$.

The result is entirely in **H**(**r**):

$$\nabla \times \left(\frac{1}{\varepsilon(r)} \nabla \times H(r)\right) = \left(\frac{\omega}{c}\right)^2 \mathbf{H}(\mathbf{r}) \qquad (2.6)$$

This is the master equation. Together with the divergence equation (2.4), it tells us everything we need to know about **H**(**r**). [1]

For a given structure ε(**r**), solve the master equation to find the modes **H**(**r**) and the corresponding frequencies, by considering transversality condition also. Using the second equation of (2.5) to recover **E**(**r**):

$$\mathbf{E}(\mathbf{r}) = i\omega\varepsilon_0\varepsilon(\mathbf{r})\,(\nabla \times \mathbf{H}(\mathbf{r})) \qquad (2.7)$$

This method ensures that **E** satisfies the transversality requirement $\nabla \cdot \varepsilon\mathbf{E} = 0$, because the divergence of a curl is always zero. Thus, we need only impose one transversality constraint. The reason why we chose to formulate the problem in terms of **H**(**r**) and not **E**(**r**) is merely one of mathematical convenience. For now, we note that we can also find **H** from **E** via the first equation of (2.5):

$$\mathbf{H}(\mathbf{r}) = -\,i\omega\mu_0\,(\nabla \times \mathbf{E}(\mathbf{r}))$$

The content of equation (2.6) states that if **H**(**r**) is an allowable electromagnetic mode, the result after the operations of the equation will just are a constant times the original function **H**(**r**). This is now a eigenvalue problem, in which **H**(**r**) is the eigenvector and $(\omega/c)^2$ is the eigenvalue .The eigenvectors **H**(**r**) are the field patterns of the harmonic modes in the dielectric material, and the eigenvalue $(\omega/c)^2$ are proportional to the squared frequencies of these modes [1]. It can also be shown that the operator $\Pi = \nabla \times \left(\frac{1}{\varepsilon(r)} \nabla \times\right)$ is linear and Hermitian. A Hermitian operator implies that the eigenfunctions (modes of different energies) are orthogonal and have real eigenvalue. If two harmonic modes have

equal frequencies ($\omega_1$ = $\omega_2$), then we say they are degenerate and not essentially orthogonal. A significant property of the electromagnetic modes is that there is no specified length scale involved. Once the eigenvalue and eigenfunctions of equation (2.6) are solved, they can be scaled to any physical size or wavelength range as long as the dielectric constant is fixed [1].

## 2.2 Periodic Dielectric Structure

Photonic crystals do not exhibit continuous translational symmetry like conventional crystals of atoms or molecules. Instead, they have discrete translational symmetry. That means they are not invariant under translations of any distance, but distances that are a multiple of some fixed step length. Lattice constant *a* is the basic step length, and the basic step vector is called the primitive lattice vector, which in this case is $\mathbf{a} = \boldsymbol{a}\,\hat{\mathbf{y}}$. Because of this discrete symmetry, $\varepsilon(\mathbf{r}) = \varepsilon(\mathbf{r} \pm \mathbf{a})$. By repeating this translation, we see that $\varepsilon(\mathbf{r}) = \varepsilon(\mathbf{r} + \mathbf{R})$ for any **R** that is an integral multiple of **a**; that is, $\mathbf{R} = l\mathbf{a}$, where *l* is an integer [22]. In this case, the Bloch-Floquet theorem for periodic eigen problems states that the solutions to Eq. (2.6) can be chosen of the form

$$\mathbf{H}(\mathbf{r}) = u_k(\mathbf{r}).\, e^{i(k.\mathbf{r})} \tag{2.7}$$

with eigenvalues of $\omega_n(\mathbf{k})$ where $u_k$ is periodic envelope function on the lattice $u_k(\mathbf{r}) = u_k(\mathbf{r} + \mathbf{R})$ for all lattice vectors R

$$(i\mathrm{k} + \nabla) \times \left(\frac{1}{\epsilon(\mathbf{r})}\,(i\mathrm{k} + \nabla) \times u_{n,\boldsymbol{k}}(\mathbf{r})\right) = \left(\frac{\omega(\mathrm{n},\mathbf{k})}{c}\right)^2 u_{n,\boldsymbol{k}}(\mathbf{r}) \tag{2.8}$$

It provides different Hermitian eigen problem which is subject to the periodic boundary condition leading to eigenvectors $u_{n,\boldsymbol{k}}(\mathbf{r})$ and eigen values $(\omega(\mathrm{n},\mathbf{k})/c)^2$. These eigenvalues are continuous functions of each Bloch wavevector **k**, which forms discrete bands, where *n* denotes the discrete eigenvalues. There are *n* solutions with frequencies $\omega_n(\mathbf{k})$ for every predetermined value of **k**. The relations $\omega_n(\mathbf{k})$ as a function of **k** comprises the photonic band structure. The photonic band structure or dispersion diagram provides us the information that we require to predict the optical properties of a photonic crystal. Moreover, the eigen solutions $u_{\boldsymbol{k}}(\mathbf{r})$ are periodic functions of **k** as well: the solution $u_{\boldsymbol{k}}(\mathbf{r})$ is same as $u_{\boldsymbol{k}+\boldsymbol{G}}(\mathbf{r})$, where G is a primitive reciprocal lattice vector defined by

$R_i \cdot G_j = 2\pi\delta_{i;j}$ . As an outcome, the eigenvalue problem can be regarded as being limited to a single unit cell of the photonic crystal and we are required to compute only the Bloch states for **k** within the primitive cell of the reciprocal lattice, which is called the Brillouin zone. In addition, the Brillouin zone may itself have rotational symmetries in the lattice, which results in additional redundancies in the solutions within the Brillouin zone corresponding to the lattice symmetries. By eliminating the redundant regions within the Brillouin zone, we obtain a zone for which the $\omega_n(\mathbf{k})$ are not related by symmetry, namely the irreducible Brillouin zone. From the rotational symmetries of the two lattice configurations we observe that the irreducible zones are fractions of the area of the full Brillouin zone. To study the dispersion properties of photonic crystals, we can bound ourselves to one period, which is usually chosen as $-\pi/a < k_z < \pi/a$, this is called as first Brillouin zone [22]. Plane waves of different directions make an orthogonal basis, and any optical wave that solves Maxwell's equation can be shown as their linear superposition. Propagation of a plane wave is entirely described by two quantities: the wave vector **k** and the optical frequency ω.

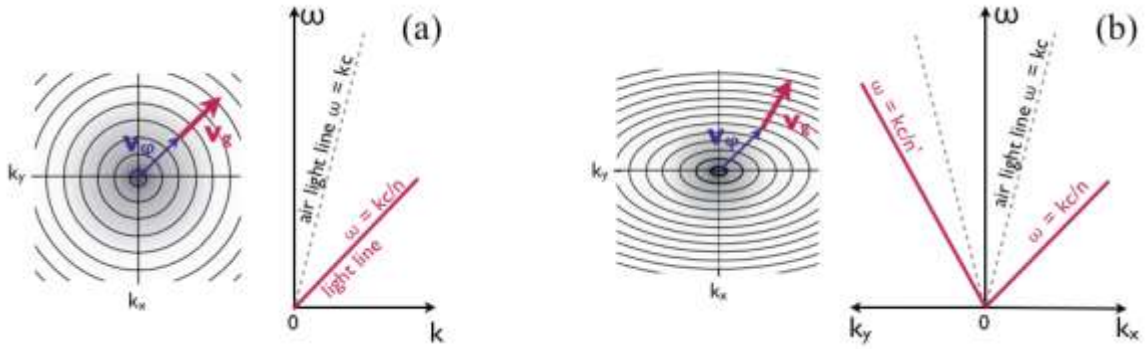


Figure 2.1: Two-dimensional dispersion map and projected dispersion diagram of (a) homogeneous isotropic and (b) anisotropic dielectric [23].

The direction of **k** determines the direction of propagation of the plane wave and the optical frequency divided by the norm of **k** defines its phase velocity [23]:

$$v_\varphi = \frac{\mathbf{k}}{k}\frac{\omega}{k} \tag{2.9}$$

The *k* and ω are linked by dispersion relation and are not constant

$$\omega = k\, v_\varphi = k\, \frac{c}{n} \tag{2.10}$$

where *c* is the velocity of light and *n* index of refraction. In an isotropic medium such as free space, the dispersion doesn't depend on the direction of propagation. Thus dispersion relation can be represented by a one dimensional plot $\omega = f(k)$ as is graphically illustrated in Fig. 2.1(a). For each frequency ω, there is just one **k** and one phase velocity equal to $v_\varphi = c/n$. The corresponding linear dispersion relation $\omega = kc/n$ is called the light line. However, in an anisotropic medium the phase velocity is depended on the propagation direction. The corresponding 2D dispersion map is shown in Fig. 2.1(b). Besides the phase velocity, we can also define the group velocity as a gradient of the optical frequency in respect to **k** [23, 25]:

$$v_g = \frac{d\omega}{dk} \tag{2.11}$$

In a medium without losses, group velocity gives the velocity of the energy transport and the direction, or we can also say that it provides the direction and velocity of propagation of optical information carried by a wave packet. It is given by the slope of the dispersion curve thus more flatter is the curve smaller is the group velocity. Its direction is always perpendicular to iso-frequency contours $\omega(\mathbf{k})$ = constant as depicted in Fig. 2.1. In non-dispersive homogeneous dielectric the group and phase velocity are same. In a general dielectric, weak deviation from the strict dispersion relation is feasible due to material dispersion $n = n(\omega)$ and the norm of the group velocity can turn out to be slightly larger or smaller than the $v_\varphi$. However, as long as the dielectric is isotropic, the directions of the two velocities are the similar in spite of the material dispersion [23].

### 2.2.1 Photonic Bandgap

When the light cannot propagate through the structure for range of frequencies then it is termed as photonic bandgap. To completely understand the concept of light propagation in a photonic crystal, we can compare it to the movement of electrons and holes inside a semiconductor [1, 24]. In a crystal, the atoms are set in a diamond-lattice structure. When electrons moves through this structure then the lattice experiences a periodic potential due to their interaction with the silicon nuclei. This interaction leads to formation of allowed and forbidden energy levels. Electrons can have energy lying in the the forbidden band if

the symmetry of the lattice is broken by a omitted silicon atom or by an impurity atom residing on a silicon site, or due to presence of interstitial impurities. If we consider movement of photons through a block of transparent dielectric material containing a number of tiny air holes which are arranged in a lattice pattern. The photons will move through regions of high and low refractive index. Contrast in refractive index to the photon will appear identical to the periodic potential that an electron experiences while travelling through a silicon crystal. If the contrast in refractive index between the two regions is large then most of the light will be confined either within the air holes or dielectric material. This results in the creation of allowed energy regions alienated by a forbidden region of photonic bandgap. The patterned dielectric material will block light for the wavelengths lying in the photonic bandgap, while it will allow other wavelengths to pass freely under certain conditions. Energy levels can be created in the photonic bandgap by introduction of a particular form of doping by altering the size of a few of air holes in the material. This is the photonic counterpart to breaking the perfect symmetry of the silicon-crystal lattice. The diameter of the air holes and refractive index contrast all through the material are critical parameters. Photonic bandgap structures can also be prepared from a lattice of high-refractive-index material entrenched within a medium with a lower refractive index. An example of such material is opal in which the contrast in the refractive index in opal is quite small which outcome in a rather small band gap [24].

## 2.3 One-Dimensional Photonic Crystal

The simplest photonic crystal consists of alternating layers of dielectric material, the known “quarter-wave-stack” as shown in Fig 2.2. When light of the proper wavelength is incident on such a layered material, it is completely reflected thus photonic crystal acts as a perfect mirror. As light wave is incident, and if the spacing is correct it is scattered at the layer interfaces also the multiply-scattered waves interfere destructively inside the material. This forms the foundation of many extensively used optical devices, such as in dielectric mirrors and dielectric Fabry-Perot filters. All enclose low-loss dielectrics that are periodic in one dimension, so they are defined one-dimensional photonic crystals [22]. However, such mirrors merely reflect light at normal or near-normal incidence to the layered material.

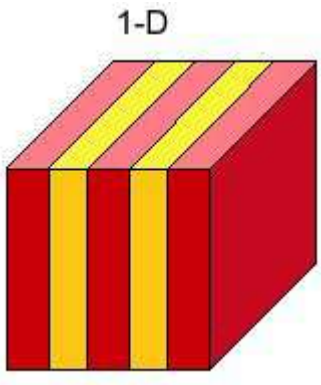


Figure 2.2: One-dimensional photonic crystal which consists of alternating layers of material with different dielectric constants which are spaced by a distance *a* [22].

### 2.3.1 Defects in one-dimensional Photonic Crystals

Translational symmetry is broken by creating a defect in one-dimensional photonic crystal by either increasing or decreasing the thickness of one of the alternating stacks of dielectric layer. The defect creates a localized mode, called a defect mode, which exist with frequency inside photonic band gap. This property forms the basis of the band-pass filter known as the dielectric Fabry-Perot filter [22].

## 2.4 Two-Dimensional Photonic Crystal

The photonic crystals in two dimensions (2D) can be understood by considering the fact that the field in every two-dimensional photonic crystals can be divided into two polarizations: TM (transverse-magnetic), in which the magnetic field is in the (xy) plane and the electric field is perpendicular (z); and the TE (transverse-electric), in which the electric field is in the plane and magnetic field is perpendicular. From Bloch's theorem and by considering that the system has discrete translational symmetry in the xy-plane, we can index the modes of the crystal by $k_z$ and $\mathbf{k}_{//}$ and n (band number) [22]:

$$\mathbf{H}_{(n,\, kz,\, \mathbf{k}//)}(\mathbf{r}) = e^{i(\mathbf{k}//.\rho)}\, e^{i(k_z .z)}.\, \mathbf{u}_{(n,\, kz,\, \mathbf{k}//)}(\rho) \qquad (2.12)$$

where $u(\rho)$ is a periodic function, $u(\rho) = u(\rho + \mathbf{R})$, for all lattice vectors **R**. Here $\mathbf{k}_{//}$ is restricted to the Brillouin zone and $k_z$ is unrestricted. The band structures for TE and TM modes can be entirely different; specifically there can be photonic band gaps for one and not for the other. Corresponding to the polarizations, there are two fundamental

topologies for two-dimensional photonic crystal. From fig. 2.3 we can observe both topologies, in the top view high refractive index rods surrounded by low index, and low-index holes in high index in the bottom view. The rods are best suited to TM light (E parallel to the rods), and the holes are best suited to TE light (E running around the holes). The basis for that is the fact that a photonic band gap requires electric field lines running along veins. Conventionally, frequencies (ω) are given in units of $2\pi c/a$, which is equivalent to $a/\lambda$ ($\lambda$ being the vacuum wavelength), as Maxwell's equations are scale-invariant, and the same explanation can be applied to any wavelength merely by choosing the appropriate *a*. Actually, hole lattice produces a complete photonic band gap (for both polarizations) not just a TE gap [22].

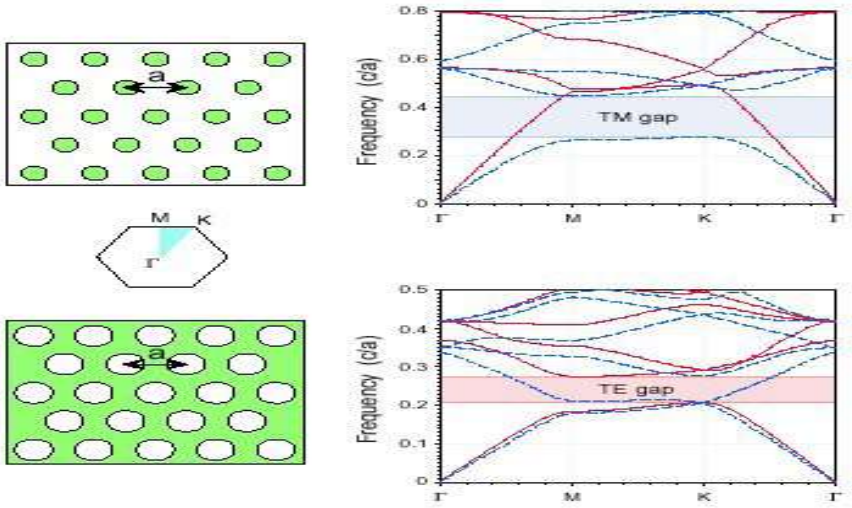


Figure 2.3: Band diagrams and photonic band gaps for hexagonal lattices of high dielectric rods ($\epsilon$= 12, r=0.2*a*) in air (top) and air holes (r=0.3*a*) in dielectric (bottom), where *a* is the lattice constant [22].

### 2.4.1 Defects in Two-dimensional Photonic Crystals

Generally in a two-dimensional photonic crystal no modes are allowed with frequencies within the gap. But by perturbing a single lattice site, we can allow a single (localized) mode that has frequency inside the gap. In two-dimensional photonic crystal we have several options to introduce defects. We can take out a single column from the crystal, or substitute it with another whose shape, size or dielectric constant is dissimilar than the original. A mode with the frequency lying in the photonic band gap becomes localized at the defect. It decays exponentially away from the defect and thus we create a cavity that is surrounded by reflecting walls and light cannot get away from it [26, 27]. These modes could be determined by a supercell approximation method. In two dimensions, we can also create linear defect by removing row of columns from the crystal. This linear defect

will guide light from one location to another. The two-dimensional array of periodic columns which enclose the line defect creates the photonic band gap. The mode that couples to the defect has a frequency which is inside the gap and light wave with this frequency is prohibited from propagating anywhere else in the structure. Although guiding in the plane of propagation is due to the photonic crystal, but in the third direction light is confined due to index contrast which exists between the slab and surrounding media [28].

## 2.5 Three-Dimensional Photonic Crystals

If a complete photonic band gap exists for some frequency range then a photonic crystal reflects light of any polarization incident at any angle. No light modes can propagate inside such crystal, if they have a frequency that lies within that range. If we can arrange contrasting dielectrics in a lattice that is periodic along three axes then only complete photonic bandgap will exist otherwise a simple dielectric mirror cannot have a complete photonic band gap. This idea of creation of a crystal of a three-dimensional lattice of dielectric spheres is still in progress. Their fabrication at sub-micrometric scales is complex to realize and not flexible enough to allow introduction of line and point defect [22].

## 2.6 Two Dimensional (2D) Slab Structure

2D slab structure has properties very similar to the ideal 2D structure. In 2D structure total internal reflection is used to guide light in the vertical direction. This shown in Fig. 2.4 structure is presented in which the thickness of the slab is $h = 0.5a$.

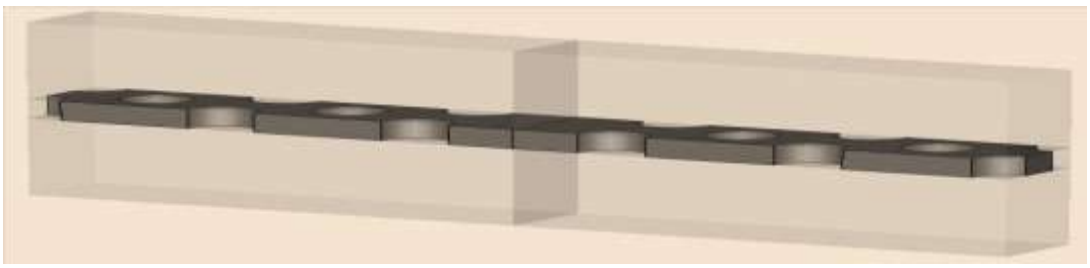

Figure 2.4: Periodic unit of 2D slab line-defect waveguide with air cladding above and below the slab and the slab has finite thickness h = 0.5*a*. The mode propagates along z axis [25].

In this structure single mode exists but at the same time light is strongly confined in the material. Below and above the slab adequate air cladding is attached so that light cannot

escape out. The boundaries of the simulation volume should be suitably away from the waveguide center in *x* and *y* directions. Here conductor boundary conditions are applicable to these boundary planes. 2D slab modes penetrate into air claddings and they propagate successfully in the medium with smaller refractive index. The main distinction is the form of the radiation modes above the $\omega = k$ line, also called light line. The modes above the light line do not complete the total internal reflection provision and are scattered vertically. Thus only the modes below the light line exist in the 2D slab structure.

## 2.7 Dispersion in Optical Waveguide

Dispersion is the phenomenon in optics in which the phase velocity of a wave depends upon its frequency, or otherwise when the group velocity depends upon the frequency. Media with such characteristics are called as dispersive media. Dispersion is often called chromatic dispersion to indicate its wavelength-dependent nature, or group-velocity dispersion (GVD) to indicate the performance of the group velocity. Group velocity dispersion causes pulses spreading in optical domain, and this spreading degrades the signals over long distances. Cancellation also takes place among group-velocity dispersion and nonlinear effects which results in occurrence soliton wave propagation. Dispersion is most repeatedly describe for light waves, but it might occur for any kind of wave that interacts with a medium or traverse through an inhomogeneous geometry like waveguide such as sound waves [29].

There are normally two sources of dispersion: waveguide dispersion and material dispersion. Frequency-dependent response of a material to waves causes material dispersion. For example, material dispersion leads to undesired chromatic aberration in a lens. In case of material dispersion different wavelengths of light travels with different velocities. If we consider a pulse that has a finite spectral bandwidth and this pulse is launched in a dispersive material then each wavelength component of the pulse will move at a different velocity. The pulse effectively disperses out in time domain and space. It will confirm that all finite temporal pulses should also have a finite frequency bandwidth. When the speed of a wave in a waveguide (such as two dimensional photonic crystal slab) is dependent upon its frequency but independent of frequency of the materials from which it is constructed then we can say that waveguide dispersion has occurred. Mostly

waveguide dispersion occurs for waves propagating all the way through any inhomogeneous structure such as photonic crystal. Generally, both types of dispersion might be there but they are not strictly accumulative in nature. Their combination results in degradation of signal in waveguides and optical fibers for telecommunications, as each signal component will have different delay and they reaches on destination at different time [29].

## 2.8 Group Velocity Dispersion (GVD)

The group velocity $v_g$ is frequently considered as it is the velocity at which energy and information is transmitted along the wave. It is true for most of the cases and the group velocity can be taken as the signal velocity of the waveform.

In case of anomalous dispersion, the rate of change of the refractive index with respect to the wavelength changes sign and in such case it is likely for the group velocity to go beyond the speed of light ($v_g > c$). Anomalous dispersion exists, for condition, where the wavelength of the light is close to an absorption resonance of the medium. When the anomalous dispersion occurs group velocity is no longer the signal velocity. Signal now travels at the speed of the wave front, which is *c* devoid of the index of refraction. Lately, it has become feasible to create gases with negative group velocity. In these cases, a pulse can appear to exit a medium before entering in it. As verified by Stenner [29] there are some cases in which chiefly a signal travels at or less than the velocity of light. The group velocity is generally a function of the wave's frequency. This results in group velocity dispersion (GVD). GVD causes spreading of short pulse of light in time as different frequency components of the pulse travel at different velocities. These components will arrive at receiver end at different times; effectively broadening signal arrival time. This effect is called group velocity dispersion (GVD).

Let us consider the case of an optical pulse which attains a finite spectral bandwidth $\Delta\lambda$ while traversing through a dispersive medium. The time which is necessary to travel a distance *L* is called the latency [30].

$$\tau = \frac{L}{c} n_g(\lambda) \tag{2.13}$$

The spectral width of the pulse ranges from $\lambda$ 1 to $\lambda$ 2 (where $\Delta\lambda$ = | $\lambda$ 1- $\lambda$ 2|).

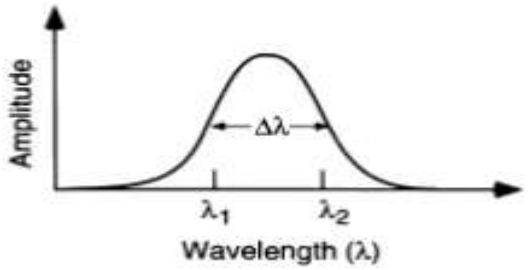


Figure.2.5: An optical pulse with a finite spread in wavelength [30].

Every signal component propagates at different velocity. Pulse spreading in time domain will be given as

$$\Delta\tau = \frac{L}{c}(n_g(\lambda 1) - n_g(\lambda 2)) \tag{2.14}$$

$$= \frac{L}{c}\Delta n_g \tag{2.15}$$

$$= \frac{L}{c}\frac{dn_g}{d\lambda}\Delta\lambda \tag{2.16}$$

Group index can be defined in terms of wavelength, and is given as

$$n_g = n - \omega\frac{dn}{d\omega} \tag{2.17}$$

On taking first derivative of equation (2.17) we can obtain $\frac{dn_g}{d\lambda}$, on putting the value of it back in equation (2.16) we can obtain pulse arrival time as below

$$\Delta\tau = -\frac{L}{c}\lambda\frac{d^2n}{d\lambda^2}\Delta\lambda \tag{2.18}$$

The pulse spreading depends upon second derivative of material dispersion thus GVD given by [30]:

$$D = -\frac{\lambda}{c}\frac{d^2n}{d\lambda^2} \tag{2.19}$$

If D is less than zero then the medium is supposed to have positive dispersion. If D is greater than zero, the medium is supposed to have negative dispersion. If a light pulse is travelling through dispersive medium, as a consequence components with higher frequency travel slower in comparison to the lower frequency components. The pulse consequently becomes positively chirped, or up-chirped, with increased frequency with time. On the Contrary, if a pulse propagates through an anomalously dispersive medium then high frequency components will travel faster than lower frequency components and the pulse becomes negatively chirped, or down-chirped, causing decreased frequency with time.

Another way of understanding the dependence of group velocity on frequency is by the GVD parameter $\beta_2$, given by second order differentiation of dispersion relation [31]. It is given as,

$$\beta_2 = \frac{d^2k}{d\omega^2} = \frac{1}{c}\frac{dn_g}{d\omega} \tag{2.20}$$

Positive or negative GVD ultimately the result is spreading of the pulse in time domain. Dispersion management is particularly important in optical communication systems based on optical waveguides and optical fibers too. High dispersion limits the length of systems and due to that signal cannot be sent on optical communication systems without regeneration. One probable solution to this issue is to send signals through fibers and waveguides at a wavelength where the GVD is zero, so pulses at this wavelength experiences minimum spreading from dispersion. But this methodology causes more problems instead of providing solution because zero GVD unfortunately leads to other nonlinear effects such as four wave mixing. Another feasible solution is to utilize soliton pulses in the regime of anomalous dispersion.

This is form of optical pulse which uses a nonlinear optical effect to self-maintain its shape. Solitons have certain practical problems such as they require a sufficient power level to be maintained in the pulse for the nonlinear effect to be occurring of the exact strength. Instead, the solution that is currently used practically is dispersion

compensation, specifically by matching the waveguide with another waveguide of opposite-sign dispersion so that the dispersion effects cancel out in each other. Such compensation is basically limited by nonlinear effects such as self-phase modulation, which interact with dispersion to make it very difficult to alter [30].

# CHAPTER 3

# Literature Survey

The simplest achievable photonic crystal consists of alternating layers of material with different index of refraction or dielectric constants. Lord Rayleigh in 1887 presented analysis of optical properties of multilayer films. This type of photonic crystal is capable of acting as a mirror (a Bragg mirror) for light with a frequency within a specified range, and light modes can also be localized by creating defects in its structure. These concepts are generally used in dielectric mirrors and optical filters (as in, e.g., Hecht and Zajac, 1997). The conventional way to evaluate this system, pioneered by Lord Rayleigh (1917), is to visualize plane wave propagation through the material and also consider multiple reflections and refractions that take place at each interface. Some of the Research methodologies developed in the field of photonic crystal waveguides are presented below:

Amnon Yariv, *et al.* in June 1999 [13] proposed optical waveguide design that consists of a series of coupled high-Q resonators (CROW). Dispersion relations and group velocity were also calculated and it was found that photonic band of proposed design is characterized by coupling factor k1. They also showed the possibility of extremely efficient nonlinear optical frequency conversion and perfect transmission through bends in CROW's.

N. Moll, *et al.* in May 2003 [32] investigated Butt coupling into photonic crystal waveguides for a two-dimensional photonic crystal and three-dimensional photonic crystal slab of a silicon-on-insulator substrate with a triangular array of holes. The transmission spectrum for both was calculated and was found to be significantly different for both. The slab system allows only a small range of frequencies in which a guided mode can exist. Butt coupling was also studied for photonic crystal waveguide (2D system) and a 3D slab system and it was concluded that a 2D calculation is not adequate to describe a slab system for all frequencies. However, using 2D calculations one might be able to identify configurations that could be appropriate in slab calculations. Their results show that complete 3D computations have to be performed to obtain quantitative results for slab systems.

C. J. Chang-Hasnain, *et al.* in December 2006 [33] discussed about recent progresses on fast and slow light using semiconductor quantum well and quantum dot devices. They demonstrated both electrical and optical controls of slow light in frequency as well as time domain. Also issues such as improvement in delay-bandwidth product need to be resolved for future practical applications.

L. Frandsen, *et al.* in December 2006 [34] demonstrated the concept for tailoring the group velocity and dispersion properties for light propagating in a planar photonic crystal waveguide. It is possible to enhance the useful bandwidth below the light-line and attain a photonic crystal waveguide with vanishing, positive, or negative group velocity dispersion by perturbing the holes adjacent to the waveguide core. Such waveguides present novel possibilities for realizing compact integrated components used for e.g. dispersion, pulse shaping.

Fengnian Xia, *et al*. in December 2006 [35] presented on-chip optical delay line based waveguide that consisted of large number of micro ring resonators which were cascaded in either coupled-resonator or all-pass filter (APF) configurations. They also analyzed trade-offs between resonantly enhanced group delay, device size, insertion loss and operational bandwidth for various delay-line designs.

T. F. Krauss in 2007 [21] discuss about the physical principles and practical limitation of slow light propagation in photonic crystal waveguides. Slow light effects in photonic crystal waveguides are most advantageously deployed to increase linear effects, such as thermo-optic and electro-optic tuning as well as gain and nonlinear effects such as Raman amplification, Kerr-based switching and possibly parametric effects such as wavelength conversion, delay lines are also possible. Broadband and slow light enhanced all-optical functions such as switches and modulators can be realized by careful device design to overcome the dispersion limitation by creating a broadband linear response, to avoid the backscattering losses encountered at the band-edge and to inject light efficiently.

L. O'Faolain, *et al.* in 2007 [38] present the effects of introducing in photonic crystal waveguides disorder on propagation loss as a function of group velocity. When disorder is deliberately introduced in controlled manner then it becomes possible to clearly

distinguish two types of losses and its contribution is presented both by simulation and experiment. A very dramatic increase in loss near the mode cut-off is observed.

J. Li, *et al.* in 2008 [37] present a systematic procedure for designing flat band photonic crystal (PhC) waveguide for slow light propagation. The method aims to maximize the group index bandwidth product by varying the position of the first two rows of holes of line defect photonic crystal waveguides. This approach has the technological advantage over keeping the hole size constant across the device as it is usually observed during etching that features such as sidewall angle can fluctuate with hole size. This effect is an important factor in minimizing propagation loss in slow light PhCs. Altering hole position might also be implemented with improved control than varying the hole size.

T. F. Krauss in 2008 [38] present in this article properties and need of slow light in various applications. Slow light offers stronger light–matter interaction along with additional control over the spectral bandwidth of this interaction and it also allows us to delay and momentarily store light in all-optical memories. He discussed about various potential devices based on optical nonlinearities, optical switching and in quantum optics. The two main challenges in a slow light structure are delay bandwidth product and dispersion. While many challenges exist, especially in optical storage but the slow-light enhancement of non linear and linear functions seems to be advancing rapidly.

E.F. Burmeister, *et al.* in 2007 [39] describe the practical and basic limitations of three optical buffering approaches and was found to be mainly due to component complexity and scalability. The architectural implementation and needs of an optical packet switch are used as a base. They investigated a range of designs to realize a recirculating optical packet buffer. Recirculating buffers with SOA gate matrix switches fulfill all requirements and present a compact solution with numerous architectural advantages.

C. Monat, *et al.* in 2009 [40] present thorough discussion on various nonlinear effects undergone by picosecond-pulses propagating through different silicon PhC waveguides of same length. The evaluation of the respective output spectral signatures all the way through fast and slow waveguides reveals an enhancement of the self phase modulation induced spectral broadening. The observed enhancement is still reduced by the immediate reinforcement of two photon absorption and free charges in the slow light regime. It is

attested by both the increased blue shift of the pulses and output power saturation arising from slower waveguides. In particular, both experimental and simulated results emphasize on the role of two photon absorption and free carriers in the silicon waveguides.

A. Melloni, *et al.* in 2010 [41] present direct comparison between photonic crystal waveguides (PhCWs) and coupled resonator optical waveguides (CROWs) as tunable delay lines. The two structures were fabricated on the identical silicon-on insulator (SOI) platform, with similar fabrication facilities and evaluated under the similar signal bit-rate conditions. They compared the time-domain and frequency response of the two structures, the physical mechanism underlying the tuning of the delay, dispersion, structural disorder, the impact of CROW and the main limits induced by loss. When lower data rates, longer delays are required CROWs are the preferred domain while when data rates in the terabit range then PhCWs remains the leading technology.

H. Kurt, *et al*. in 2010 [42] present study of different spectral features such as constant group index, high bandwidth and low group velocity dispersion during propagation of slow light in monomode photonic crystal waveguides. Detailed analysis is performed to manage the dispersion. The frequency domain calculations validate that when the radii of the side rows of holes rise above certain value then distinctive properties in the waveguide mode emerge due to the interaction with continuum states. The inverse exponential relation among group index and bandwidth is explored.

Jin Hou, *et al*. in 2010 [43] present wideband zero dispersion slow light in chirped-slot photonic crystal coupled waveguide. Effects of chirping a variety of parameters and design principles to achieve the ideal chair shape of the dispersion curve are discussed. By merely chirping the widths of the photonic crystal waveguides, wideband slow light with optical confinement in the low dielectric slot is established numerically. Proposed structures would recommend significant potential for compact high speed optical signal processing devices.

R. Hao, *et al.* in 2010 [44] demonstrated slow light photonic crystal waveguide which can create unusual “U” type group index frequency curves with constant group index over large bandwidth and low group velocity dispersion. In this geometry only shifting of the

waveguide bordering rows of holes is done. Additionally, control of normalized delay-bandwidth product has been shown. The GVD properties of the proposed structure have been also analyzed. This designed waveguide allows a probable control of positive or negative GVD values, providing opportunities for dispersion compensation devices.

M. Shinkawa, *et al.* in 2011 [45] present design methodology of lattice-shifted photonic crystal waveguide which was fabricated using CMOS-compatible process which displayed low-dispersion slow light and nonlinear enhancement. Unique nonlinear response is observed some of which may be applicable for signal processing by combination of the specific transmission spectrum and nonlinearities.

Yi Zhai, *et al.* in 2011 [46] present theoretical investigation of flat band slow light in a ring shape hole photonic crystal waveguide (RPCW). Results show that both inner and outer radii of the first two rows of holes next to the defect have much effect on slow light properties. By properly varying the outer and inner radii of the ring-shaped holes slow light can be achieved. The negligible dispersion bandwidths for suitable group indices are obtained. Buffer capability and signal transmission parameters are also calculated for the RPCW. The proposed structure has substantial potential for optical buffering applications.

C. Caer, *et al*. in 2013 [47] present design of silicon on insulator wide slot photonic crystal waveguides (PCWs). Two design schemes are presented based on dispersion engineering of slot and hole lattice. Band diagrams and mode patterns are determined by 3D-plane wave expansion method. Results show high coupling efficiencies and high amplitudes interference fringes. This study provides insights for losses in hollow core slot high group index waveguides.

K. Kondo, *et al.* in 2013 [48] demonstrated way to tune the delay of the signal pulse (all optically) using two types of slow light in the lattice shifted photonic crystal waveguide (LSPCW). Two photon absorption induced carrier plasma effect gives rise to the dynamic tuning, leading to ultrafast delay tuning. It is not limited by the carrier lifetime but by the incident timing of the control pulse and device length. LSPCW could be integrated with heaters and p-n diodes, using a CMOS-compatible process and thus can be used to externally control delay characteristics, target wavelength and dispersion.

J. Tang, *et al.* in 2013 [49] presents design of photonic crystal waveguide structure by selectively altering the locations of the holes adjacent to the line defect to achieve wideband slow light with large group index and low dispersion. Low dispersion slow light propagation is assured by studying the relative temporal pulse width spreading with the two-dimension finite-difference time-domain method. These new waveguides allow a versatile control of positive or negative GVD values and reveal the possibility of dispersion-compensating applications

J. Tang, *et al.* in 2014 [50] present a systematic optimization method to generate slow light with large group index, low dispersion and wideband in an ellipse-hole photonic crystal waveguide. Bandwidth, group index and dispersion can be tuned effectively by varying the orientation of the ellipse holes in the first row and also by shifting longitudinal position of the third row of holes. Slow light with low-dispersion propagation was assured by studying the spreading of pulse width the two-dimensional finite difference time-domain method.

# CHAPTER 4

# Proposal of Slow Light In Photonic Crystal Line Defect Waveguide

## 4.1 Structure of Photonic Crystal Waveguide

Photonic crystal waveguide are normally made up by periodically patterning columns of air holes in high index material slabs. Design of photonic crystal waveguide is shown in Fig 4.1. A photonic crystal slab with high refractive index dielectric material (i.e. Si) with air-holes arranged in hexagonal array is one of the most attractive photonic crystal structures. A two dimension photonic crystal can be realized in three dimensions by taking photonic crystal slab with finite height. In such structure light can be confined vertically by total internal reflection. For an appropriate design of the waveguide some defect states are located within the band gap of the photonic crystal, so that light is confined along the line defect in the plane of the crystal in this frequency range. Combining this in-plane confinement with the vertical confinement due to the index contrast in the vertical direction, 3D light confinement is possible within a waveguide in a photonic crystal slab. If the slab thickness is not too small and the index contrast between core and cladding is not too low, there exist some states in the slab which form a photonic gap below the light line. The larger the index contrast between core and claddings, the more modes exist below the light line.

Direction of periodicity that we have considered is along the waveguide (the *x*-direction) and all the calculations are made for wave vector range $0.3 \leq k_x \leq 0.5$, as this is the region which corresponds to low group velocity. In our basic Structure A, we have considered silicon slab with refractive index of 3.48 and slab height of 220nm. Air holes with radius 0.30*a* and refractive index 1 are etched on silicon slab to height 1.001 of slab height. This height is chosen to ensure holes are etched in silicon slab properly. The lattice constant *a* is the distance between centers of holes and it is chosen to be 430 nm for both directions x and y. As the index contrast between core and cladding is very high, so light is strongly confined within the core. Because of the finite height of the slab, polarization mixing

occurs and the modes are not purely TE or TM polarized anymore. In case of a photonic crystal slab waveguide, it is convenient to define a rectangular unit cell which is indicated by the blue box in Fig. 4.1(b).

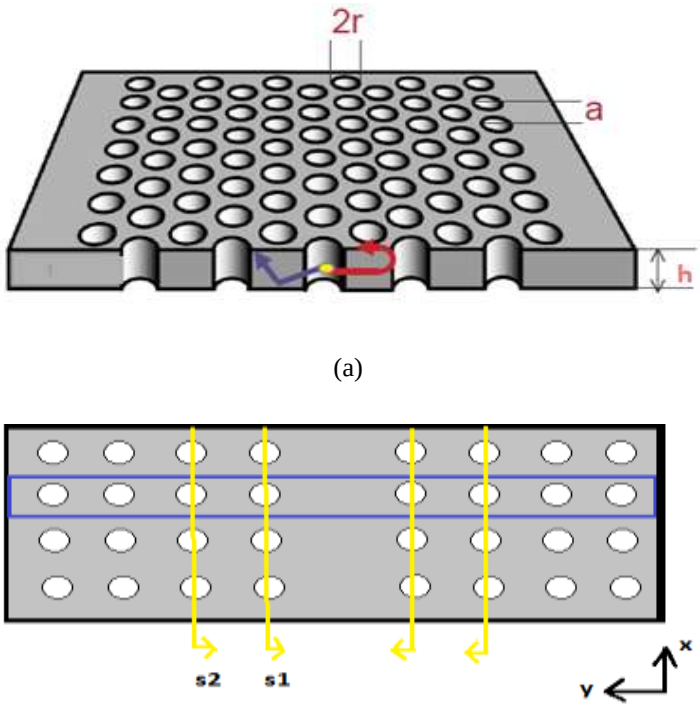


Figure 4.1(a): Geometry of photonic crystal (PC) slab waveguide with high refractive index region of silicon indicated by grey color and circular air holes of low refractive index represented by white. Air holes of radius r are etched over silicon slab of thickness h. *a* is the lattice constant which denotes distance between centers of air holes. (b) Initial design of line defect PC slab waveguide formed by removing single row of air holes. In proposed structures position of two rows of holes adjacent to waveguide is shifted by s1 and s2 amount.

### 4.1.1 Electric and Magnetic Field Profiles

Fig. 4.2 shows the electric and magnetic field pattern at $k$= 0.40 of guided band. The single line defect photonic crystal waveguide can confine light within the narrow region of high refractive index material. This line defect in the centre disturbs the periodicity of air-holes which will help in obtaining strong optical confinement in the narrow region. The periodic structure (air holes) surrounding the defect causes a collective cancellation of scattering of light leading to guiding of light in the defect region. We also observe that field of desired mode is interacting with first and second row of holes during its course of propagation and thus varying properties of these rows of holes will have significant effect

on the properties of guided band. Field profiles, Band structures, group index values are calculated using MPB software package.

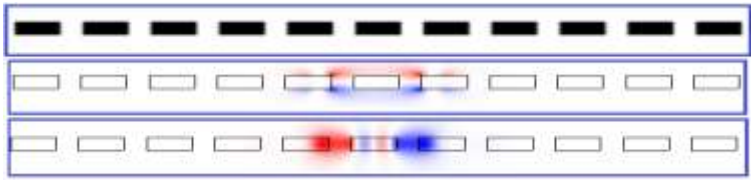

Figure 4.2: Rectangular unit cell along with its electric and magnetic field profile at $k$ =0.40.

### 4.1.2 Band Structure

The photonic band structure gives us information about the propagation properties of electromagnetic radiation within the photonic crystal. It is a representation in which the available energy states are plotted as a function of propagation direction. The relationship between the wave-vector and frequency (also known as dispersion relation) for free photons in vacuum is well known: ω=ck, where *c* is the vacuum light velocity. If photons are propagating through a homogeneous and isotropic dielectric then ω=ck/n, where n is the refractive index of the dielectric material. Fig. 4.3 shows the band diagram of Structure A which is formed by creating line defect waveguide. Air cladding light line is indicated by blue line and all the bands by different colors. Our desired band of interest is shown by dashed black line. We can observe it lies well below the air light line ensuring low radiation losses.

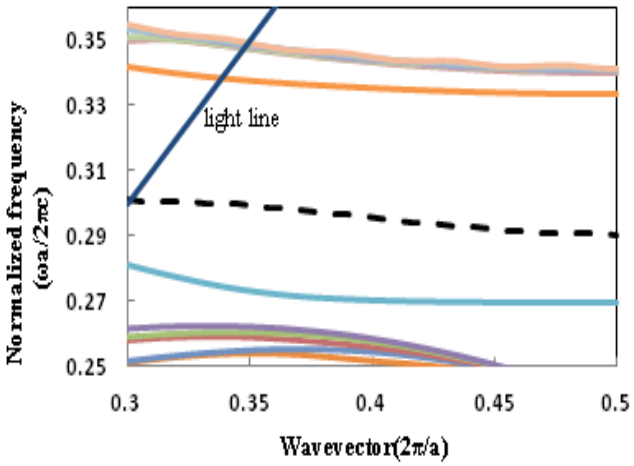


Figure 4.3: Normalized frequency vs. Wavevector curve for guided mode where *c* is the velocity of light in vacuum and *a* is the lattice constant which is taken as 430nm. Blue line is the air light line and dashed black line is the dispersion line for basic Structure A.

Relationship between group velocity $v_g$ of light and frequency is given as

$$v_g = \frac{d\omega}{dk} = \frac{c}{n_g} \tag{4.1}$$

where $k$ is the wave vector along the waveguide $n_g$ is the group index. Dependence of group velocity on frequency is identified by the GVD parameter $\beta_2$, given by second order differentiation of dispersion relation [51]

$$\beta_2 = \frac{d^2k}{d\omega^2} = \frac{1}{c}\frac{dn_g}{d\omega} \tag{4.2}$$

Delay bandwidth product is considered as figure of merit for analysing slow light performance. DBP is defined as product of group delay $\Delta t$ and bandwidth $\Delta\omega$ in slow light

$$\text{DBP} = \Delta t \,.\, \Delta\omega \tag{4.3}$$

However, normalized delay bandwidth product (NDBP) is used when we want to compare structures of different lengths and it is given as [40]

$$\text{NDBP} = \hat{n}_g \,.\, \Delta\omega / \omega_0 \tag{4.4}$$

where $\omega_0$ is the normalized central frequency of the light wave and $\hat{n}_g$ is average group index measured over bandwidth $\Delta\omega$ in which variation of $n_g$ is within ±10% [31, 34, 52]. From eq. (4.4) we can observe that in order to achieve high NDBP values it is necessary to increase bandwidth in flat band slow light region while maintaining high group index values and linear dispersion curve.

### 4.1.3 Group Index Characteristics of Initial Design

Group index characteristics for Structure A are shown in Fig. 4.4. Here we can see that group index values as high as 180 is obtained but there is no flat band region. Flat region we have considered is the one with variation of $n_g$ within ±10%. We know that flatter is the group index curve lower is the group velocity dispersion. Flat band is observed for

very low group index values of around 10 but these are not of our interest as our aim is to achieve slow light with high group index values and low group velocity dispersion.

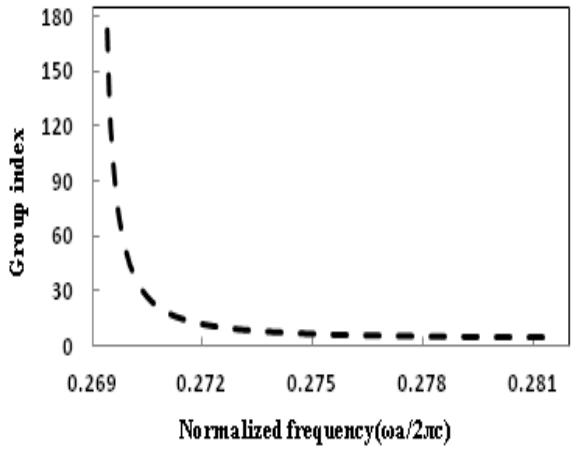


Figure 4.4: Group index vs. Normalized frequency plot for Structure A with no shifting of rows of holes adjacent to defect waveguide.

Fig 4.5 shows group index (dashed) and group velocity (dotted) as function of wavelength. Group velocity as low as 0.005*c* for group index of 180 at wavelength 1596 nm is observed but as we do not obtain any flat band region for such high group index value in this Structure so even this much high value of group index is of no practical usage. Group velocity for the flatter region lies in the range of 0.08*c* to 0.20*c* over wavelength 1529 nm to 1580 nm. But this region of low group velocity is not of our interest.

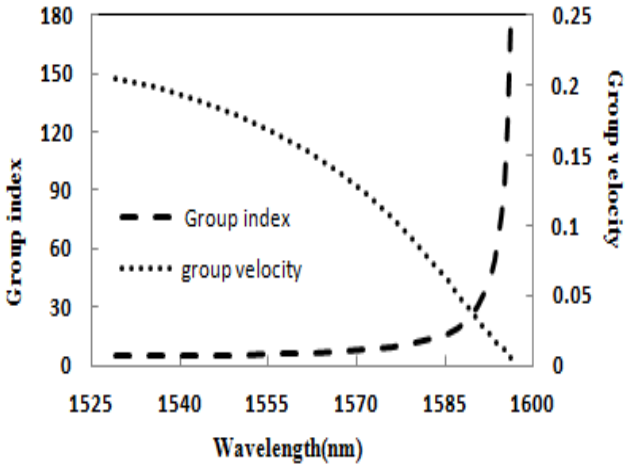


Figure 4.5: Group index and Group velocity vs. Wavelength (nm) characteristics for Structure A. Dashed and dotted lines indicate curves for Group index and Group velocity.

### 4.1.4 Group Velocity Dispersion Parameter of Initial Design

Group velocity dispersion (GVD) is characterized by $\beta_2$ parameter and is very important as it controls the signal distortion and pulse broadening in the slow light region. Low value of GVD parameter is desired so that high group index values are not obtained at the cost of increase in signal distortion. Fig. 4.6 shows the GVD parameter as function of normalized frequency. For this Structure positive, negative and zero values of $\beta_2$ are obtained with maximum of $-7.09 \times 10^5$ $ps^2/km$ at Normalized frequency of 0.269386.

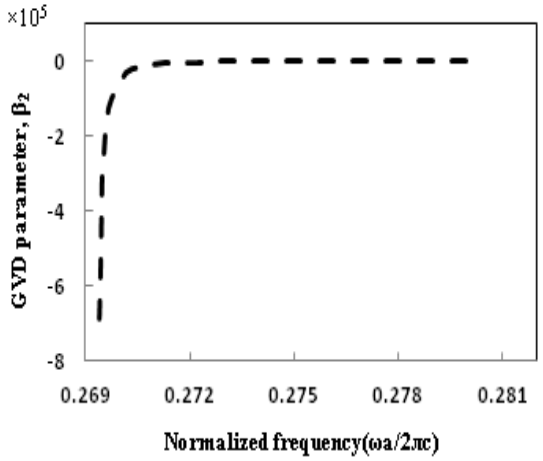


Figure 4.6: GVD parameter vs. Normalized frequency for basic Structure A.

In our proposed Structures, we are altering the width of defect line by shifting positions of two rows of holes which are adjacent to the waveguide. Controlling radius of holes at nanometer scale is very difficult from fabrication point of view thus shifting is more appropriate [37]. In different Structures we have shifted the position of first and second row of holes by s1 and s2 amount. If the amount by which first row of holes are shifted increases, than guided band will shift towards lower frequencies and if the amount by which second row of holes are shifted decreases, than guided band will shift towards higher frequencies.

## 4.2 Analysis of Structure B

In Structure B, all the parameters remain same as Structure A. First row of holes is shifted away from waveguide by 50 nm and second row of holes are shifted towards the waveguide by 10 nm. Fig. 4.7 shows Dispersion curve for Structure B along with Basic Structure A. In Structure B, s1= -50 nm and s2= -10 nm. As s1 is increased and s2 is decreased, our band of interest is shifted accordingly (shift value away from waveguide is considered as increasing value). We have obtained band gap of 9% for Normalized

frequency range from 0.287729 to 0.31583 and our band of interest in Structure B lies in this bandgap range. Photonic bandgap is often described in terms of gap-midgap ratio. Let $\omega_m$ be the frequency at the middle of the gap, thus we define gap–midgap ratio as $\Delta\omega/\omega_m$, often expressed as a percentage [1]. Gap-midgap ratio for Structure B is calculated to be 9.3%.

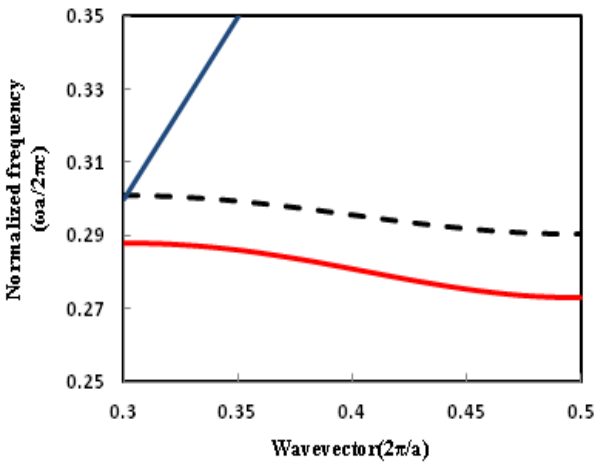


Figure 4.7: Dispersion curve for Structure B where *c* is the velocity of light in vacuum and *a* is the lattice constant which is taken as 430 nm. Blue line as the air light line and red line is the shifted band of interest from dashed black line of basic Structure A.

Fig 4.8 shows group index (red line) as function of Normalized frequency. For the frequency range 0.264389 to 0.266628 we have observed flat band region with average group index value of 44.9.

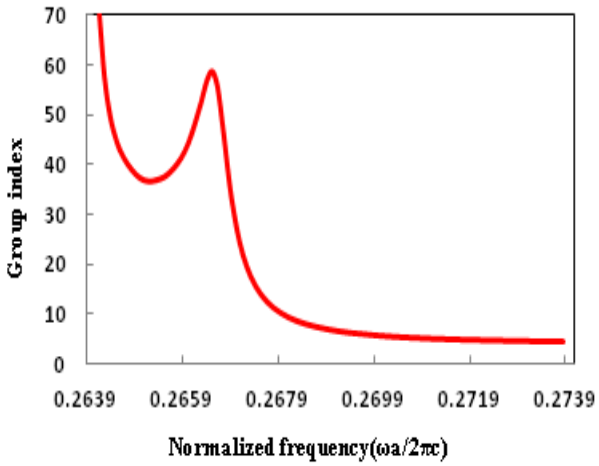


Figure 4.8: Group index vs. Normalized frequency plot for Structure B with shifting of first and second row of holes by s1 and s2 amount.

Fig. 4.9 shows group index (dashed) and group velocity (dotted) as function of wavelength. Flat band region is observed from 1612.7 nm to 1626.3 nm over a wavelength bandwidth of 13.66 nm. Group velocity in this flat band region lies between 0.018*c* to 0.020*c*.

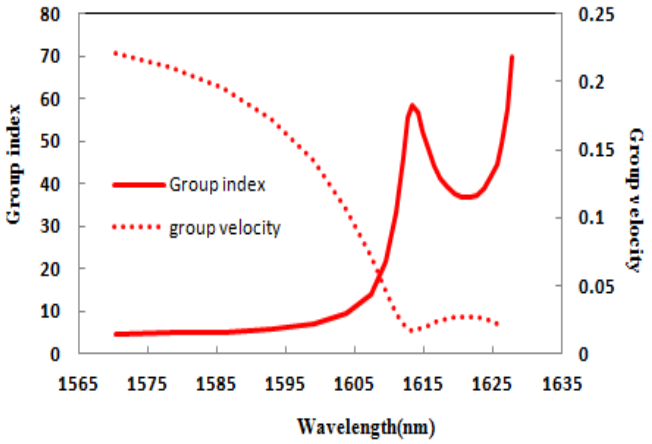


Figure 4.9: Group index and Group velocity as function of wavelength (nm) for Structure B. Dashed and dotted lines indicate curves for Group index and Group velocity.

Fig. 4.10 shows the GVD parameter as function of normalized frequency. For this Structure positive and negative values of $\beta_2$ are obtained. But its value lies in the range of $10^4$ $ps^2/km$, which is one order less than that observed in Structure A.

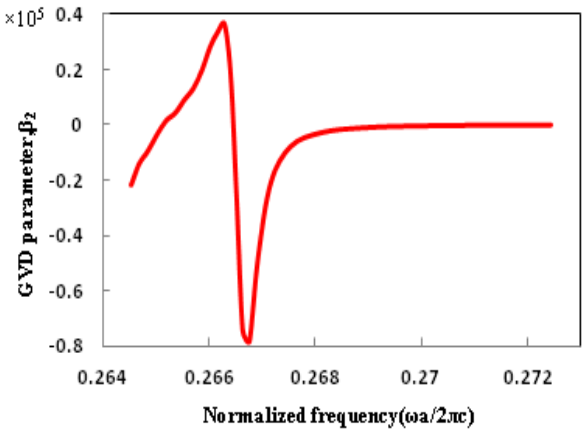


Figure 4.10: GVD parameter as function of Normalized frequency for Structure B exhibits positive as well as negative values over desired range of frequencies.

## 4.3 Analysis of Structure C

In Structure C all the parameters remains same as Structure A. First row of holes is shifted away from waveguide by 48 nm and second row of holes are shifted towards the

waveguide by 16 nm. Fig. 4.11 shows Dispersion curve for Structure C along with Basic Structure A. In Structure C, s1= -48 nm and s2= 16 nm. As s1 is increased and s2 is decreased, our band of interest is shifted accordingly (Shift value away from waveguide is considered as increasing value). We have obtained band gap of 9% for Normalized frequency range from 0.28879 to 0.31724 and our band of interest in Structure C lies in this bandgap range. Gap-midgap ratio for Structure C is calculated to be 9.3%.

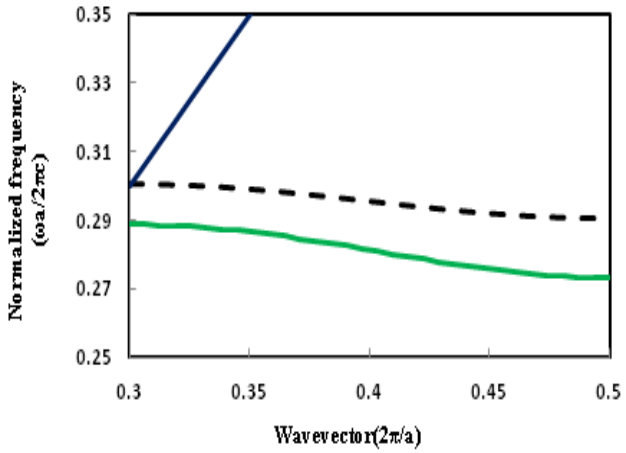


Figure 4.11: Normalized frequency vs. wavevector plot for Structure C (green line) with shifting of first and second row of holes by s1 and s2 amount ,where c is the velocity of light in vacuum and *a* is the lattice constant which is taken as 430 nm.

Fig 4.12 shows group index (green line) as function of Normalized frequency. For the frequency range 0.265345 to 0.266969 we have observed flat band region with average group index value of 53.9.

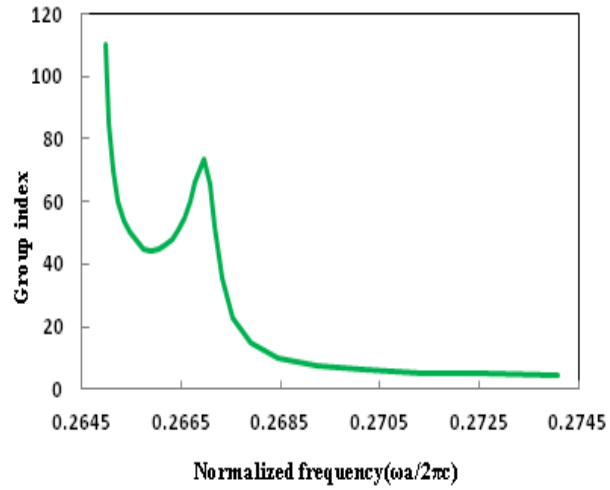


Figure 4.12: Group index vs. Normalized frequency characteristics for Structure C.

Fig. 4.13 shows group index (dashed line) and group velocity (dotted line) as function of wavelength. Flat band region is observed from 1610.7 nm to 1620.5 nm over a wavelength bandwidth of 9.858 nm. Group velocity in this flat band region lies between 0.0136*c* to 0.018*c*.

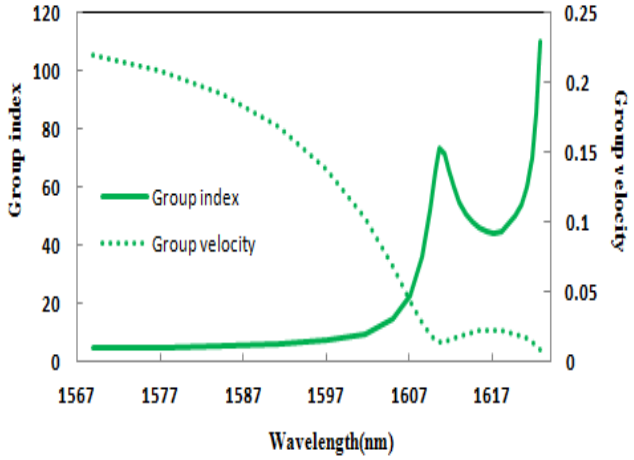


Figure 4.13: Group index and Group velocity as function of wavelength (nm) for Structure C.

Fig. 4.14 shows the GVD parameter as function of normalized frequency. For this Structure positive and negative values of $\beta_2$ are obtained. But its value lies in the range of $10^4$ $ps^2$/km, which is one order less than that observed in Structure A.

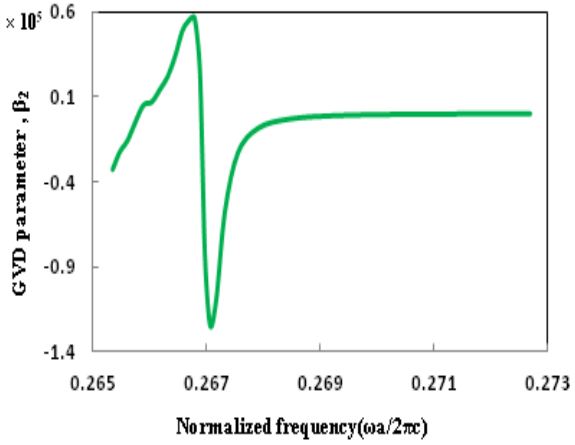


Figure 4.14: GVD parameter vs. normalized frequency for Structure C. It exhibits positive as well as negative values over desired frequency range.

## 4.4 Analysis of Structure D

In Structure D all the parameters remains same as Structure A. Only first row of holes is shifted away from waveguide by 52 nm and second row of holes remains unaltered. Fig.

4.15 shows Dispersion curve for Structure D along with Basic Structure A. We have obtained band gap of 9% for Normalized frequency range from 0.28645 to 0.31453 and our band of interest in Structure D lies in this bandgap range. Gap-midgap ratio for Structure D is calculated to be 9.3% (in terms of percentage).

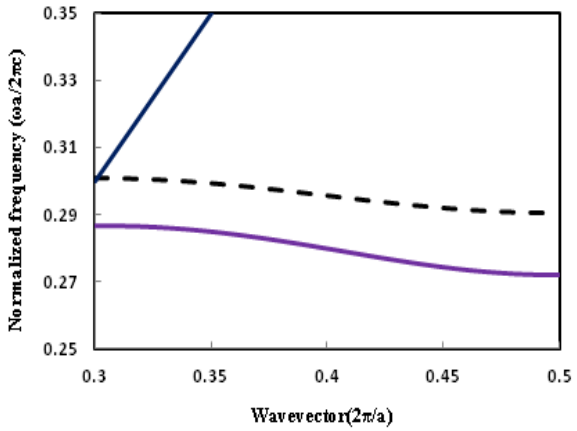


Figure 4.15: Dispersion curve for Structure D with band of interest indicated by purple line and light line by blue line. Dashed black line is the band of interest of basic Structure A.

Fig 4.16 shows group index (purple line) as function of Normalized frequency. For the frequency range 0.263349 to 0.265916 we have observed flat band region with average group index value of 36.16.

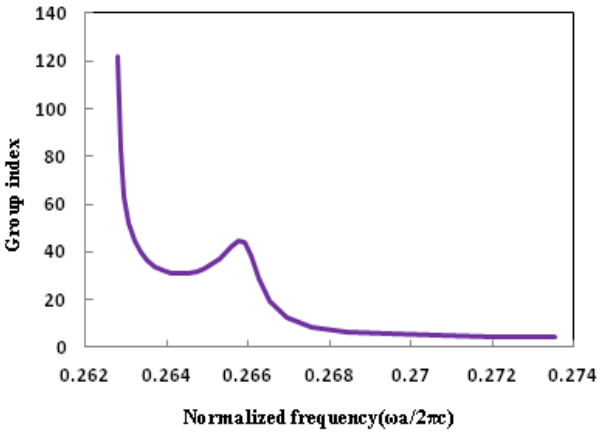


Figure 4.16: Group index vs. Normalized frequency plot for Structure D (purple line) with shifting of first and second row of holes by s1 and s2 amount ,where c is the velocity of light in vacuum and *a* is the lattice constant which is taken as 430 nm.

Fig. 4.17 shows group index and group velocity (dotted purple line) as function of wavelength. Flat band region is observed from 1617 nm to 1632.8 nm over a wavelength

bandwidth of 15.76 nm. Group velocity in this flat band region lies between 0.023*c* to 0.025*c*.

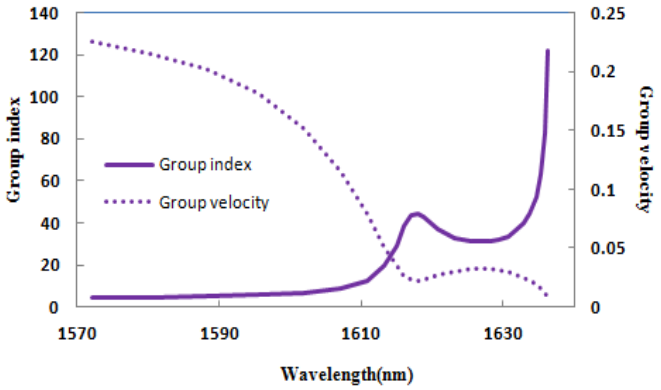


Figure 4.17: Group index and Group velocity as function of wavelength (nm) for Structure C.

Fig. 4.18 shows the GVD parameter as function of normalized frequency. For this Structure positive and negative values of $\beta_2$ are obtained. But its value lies in the range of $10^4$ $ps^2/km$, which is one order less than that observed in Structure A.

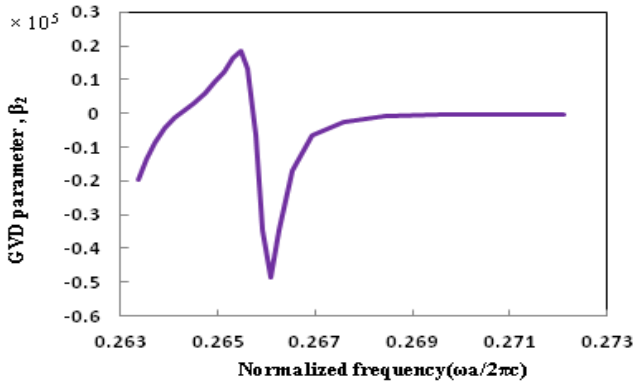


Figure 4.18: GVD parameter vs. Normalized frequency for Structure D. It exhibits positive as well as negative values over desired frequency range.

## 4.5 Modified Structures

In Structure A, B, C and D we were keeping the lattice constant value as 430 nm. However in order to have same wavelength range for all these Structures we varied lattice constant value also and named modified Structures as B', C' and D'.

### 4.5.1 Analysis of Structure B'

In Structure B' all the parameters remain same as Structure B. Lattice constant for this Structure is taken as 411.5 nm. We have obtained band gap of 9.3% for Normalized

frequency range from 0.28476 to 0.312581 and our band of interest in Structure B' lies in this bandgap range. Fig 4.19 shows group index (brown line) as function of Normalized frequency. For the frequency range 0.261619 to 0.263977 we have observed flat band region with average group index value of 46.5. Gap-midgap ratio for Structure B' is calculated to be 9.3% (in terms of percentage).

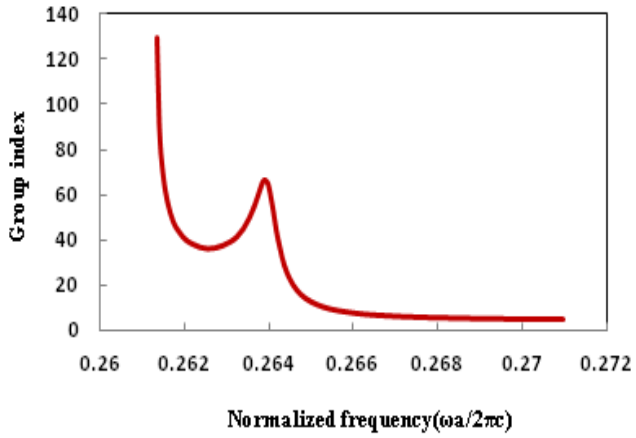


Figure 4.19: Group index vs. Normalized frequency plot for Structure B' (brown line) with shifting of first and second row of holes by s1 and s2 amount ,where *c* is the velocity of light in vacuum and *a* is the lattice constant which is taken as 411.5nm.

Fig. 4.20 shows group index and group velocity (dotted brown line) as function of wavelength. Flat band region is observed from 1558.84 nm to 1572.89 nm over a wavelength bandwidth of 14.05 nm. Group velocity in this flat band region lies between 0.015*c* to 0.0178*c*.

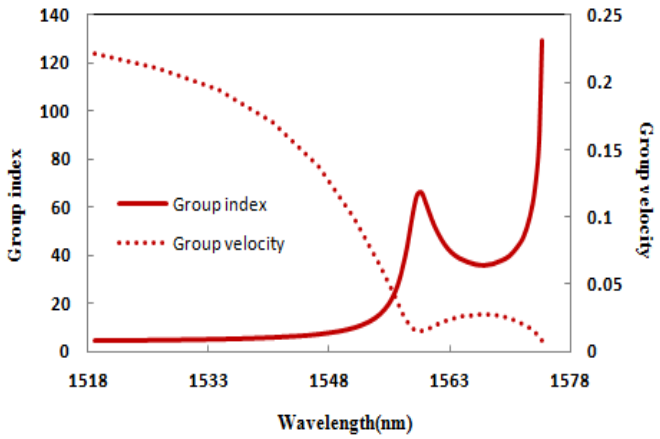


Figure 4.20: Group index and Group velocity as function of wavelength (nm) for Structure B'.

Fig. 4.21 shows the GVD parameter as function of normalized frequency. For this Structure positive and negative values of $\beta_2$ are obtained. But its value lies in the range of $10^4$ $ps^2$/km, which is one order less than that observed in Structure A.

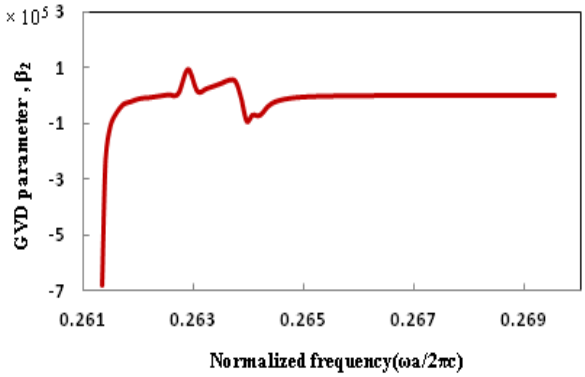


Figure 4.21: GVD parameter vs. Normalized frequency for Structure B'. It exhibits positive as well as negative values over desired frequency range.

### 4.5.2 Analysis of Structure C'

In Structure C' all the parameters remain same as Structure C. Lattice constant for this Structure is taken as 412.5 nm. We have obtained band gap of 9.3% for Normalized frequency range from 0.28596 to 0.313849 and our band of interest in Structure C' lies in this bandgap range. Fig 4.22 shows group index (yellow line) as function of Normalized frequency. For the frequency range 0.262834 to 0.264723 we have observed flat band region with average group index value of 54.58. Gap-midgap ratio for Structure C' is calculated to be 9.3% (in terms of percentage).

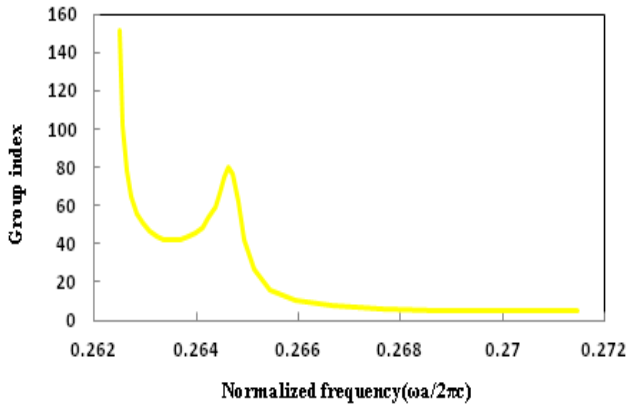


Figure 4.22: Group index vs. Normalized frequency plot for Structure C' (yellow line) with shifting of first and second row of holes by s1 and s2 amount, where *c* is the velocity of light in vacuum and *a* is the lattice constant which is taken as 412.5nm.

Fig. 4.23 shows group index and group velocity (dashed) as function of wavelength. Flat band region is observed from 1558.23 nm to 1569.4 nm over a wavelength bandwidth of 11.19 nm. Group velocity in this flat band region lies between 0.013*c* to 0.0179*c*.

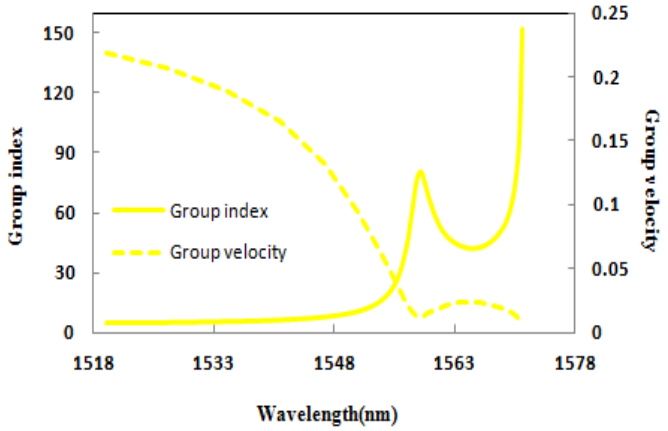


Figure 4.23: Group index (yellow line) and Group velocity (dashed yellow line) as function of wavelength (nm) for Structure B'.

Fig 4.24 shows the GVD parameter as function of normalized frequency. For this Structure positive and negative values of $\beta_2$ are obtained. But its value lies in the range of $10^4$ $ps^2/km$, which is one order less than that observed in Structure A. GVD parameter is still considered to be lying in low dispersion range.

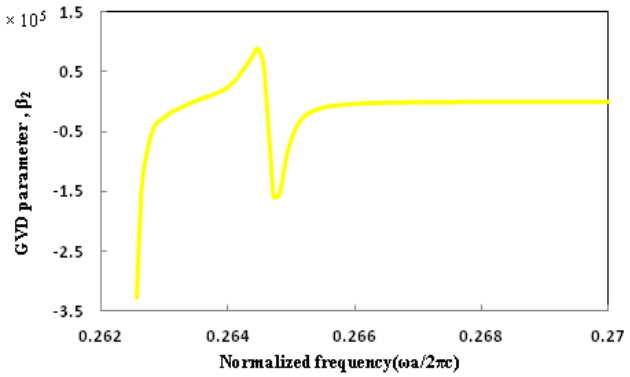


Figure 4.24: GVD parameter vs. Normalized frequency for Structure C'. It exhibits positive as well as negative values over desired frequency range.

### 4.5.3 Analysis of Structure D'

In Structure D' all the parameters remain same as Structure D. Lattice constant for this Structure is taken as 410.316 nm. We have obtained band gap of 9.3% for Normalized

frequency range from 0.283016 to 0.310625 and our band of interest in Structure D' lies in this bandgap range. Fig 4.25 shows group index (sky blue line) as a function of Normalized frequency. For the frequency range 0.260127 to 0.263268 we have observed flat band region with average group index value of 36.60. Gap-midgap ratio for Structure D' is calculated to be 9.3% (in terms of percentage).

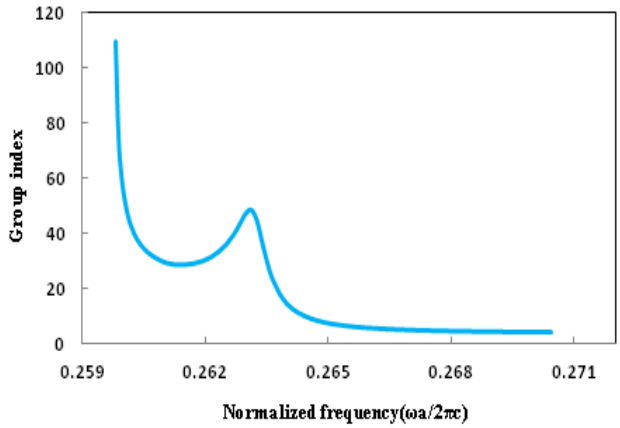


Figure 4.25: Group index vs. Normalized frequency plot for Structure C' with shifting of first and second row of holes by s1 and s2 amount, where *c* is the velocity of light in vacuum and *a* is the lattice constant which is taken as 410.316 nm.

Fig. 4.26 shows group index and group velocity (dashed sky blue line) as function of wavelength. Flat band region is observed from 1558.5 nm to 1577.36 nm over a wavelength bandwidth of 18.81 nm. Group velocity in this flat band region lies between 0.013*c* to 0.0179*c*.

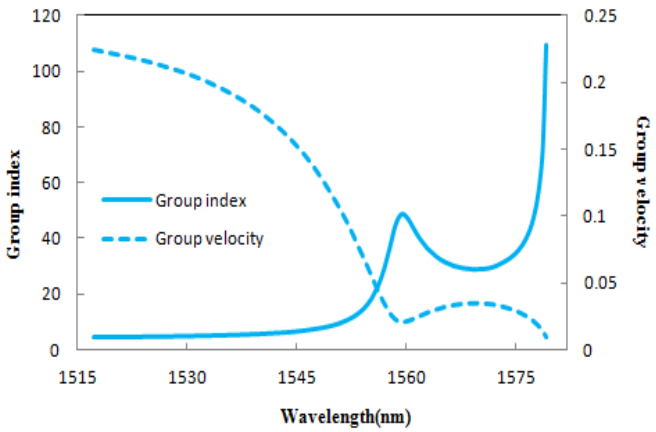


Figure 4.26: Group index (sky blue line) and Group velocity (dashed sky blue line) as function of wavelength (nm) for Structure D'.

Fig 4.27 shows the GVD parameter as function of normalized frequency. For this Structure D', positive, negative and zero values of $\beta_2$ are obtained. But its value lies in the range of $10^4$ $ps^2/km$, which is one order less than that observed in Structure A. GVD parameter is still considered to be lying in low dispersion range.

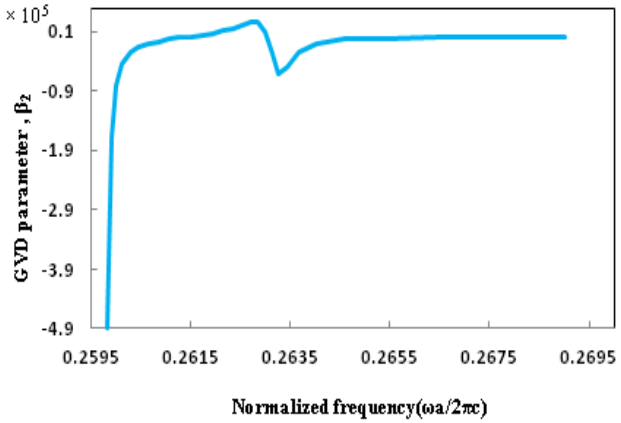


Figure 4.27: GVD parameter vs. Normalized frequency for Structure D'. It exhibits positive as well as negative values over desired frequency range.

Table 1 summarizes various design parameters we have considered and obtained for all the Structures A, B, C, D, B', C' and D'. s1 and s2 are the shift amount by which first and second row of holes are shifted. Positive and negative value indicates shifts towards and away from the defect waveguide. $\hat{n}_g$ is the average group index value over the bandwidth of interest.

Table 1 Structural Design Parameters

| Structure | $a$ (nm) | s1 | s2 | $\hat{n}_g$ | $\Delta\omega/\omega_0$ |
|---|---|---|---|---|---|
| A | 430 | 0 | 0 | - | - |
| B | 430 | -01162$a$ | 0.02325$a$ | 44.5 | $7.914\times10^{-3}$ |
| C | 430 | -0.11162$a$ | 0.0372$a$ | 53.95 | $6.1\times 10^{-3}$ |
| D | 430 | -0.12093$a$ | 0 | 36.16 | $9.64\times 10^{-3}$ |
| B' | 411.5 | -0.121506$a$ | 0.02430$a$ | 46.52 | $8.97\times 10^{-3}$ |
| C' | 412.5 | -0.11636$a$ | 0.038787$a$ | 54.58 | $7.161\times 10^{-3}$ |
| D' | 410.316 | -0.126731$a$ | 0 | 36.60 | $12\times 10^{-3}$ |

## 4.6 Applicability in Buffering

In slow light devices, dispersion, bandwidth and losses are fundamental issues to be addressed which limit its usage as buffers. Slow light buffers would degrade network performance by limiting packet length and therefore network load. High dispersion yields low bandwidth delay product. This results in impractical bit rates and capacities [39].

There are certain parameters to evaluate performance of a buffer namely storage time, buffer capacity and length per bit. If length of delay line based PC waveguide is *L*, then storage time is given as,

$$\Delta t = L / v_g = n_g \times \frac{L}{c} \quad (4.5)$$

From eq. (4.5) we can say that storage time is proportional to $n_g$ and waveguide length. However, for a waveguide with normalized length it is determined only by $n_g$ .Second parameter is buffering capacity C, which is defined as maximum number of bits device can store and is given as,

$$C = \Delta t \times B \quad (4.6)$$

where B is the bit rate. Buffer capacity is also given as [40],

$$C = \frac{L}{2a} \times n_g \times \Delta\omega \quad (4.7)$$

We can observe from eq. (4.7) that buffer capacity is proportional to group index bandwidth product. $L_{bit}$ is the physical size of each bit which is stored in buffer and thus is a limiting factor in deciding physical size of the buffer and it is given as,

$$L_{bit} = \frac{L}{c} = \frac{2a}{n_g \Delta\omega} \quad (4.8)$$

Eq. (4.8) shows that physical size is inversely proportional to group index bandwidth product and thus to increase buffer capacity and to decrease its physical length, larger value of group index bandwidth product is desired. The length of delay line is *L* is taken as 1 mm [46].

Table 2 summarizes the buffering parameters in all Structures. As group index increases, bandwidth decreases and buffering capacity also decreases. So, there is a trade-off between bandwidth and group index value. Structure C, with average group index value of 53.9, has largest $L_{bit,}$ smallest buffering capacity and storage time value of 180ps. Structure D' with average group index of 31.4, has largest bandwidth and buffering capacity with storage time of 122 ps. Structure C' has highest group index value, moderate bandwidth and largest storage time. Depending upon the application we can choose among all proposed Structures. For buffering, either Structure B' or D' will be suitable choice with buffering capacity of 134 and 140 bits.

Table 2 Buffering parameters in all Structures

| Structure | $a$(nm) | $\hat{n}_g$ | Δω ($10^{-4}$ωa/2πc) | Δλ(nm) | NDBP | Δ$t$ (ps) | $L_{\text{bit}}$ (μm) | C (bit) |
|---|---|---|---|---|---|---|---|---|
| B | 430 | 44.9 | 22.4 | 13.66 | 0.38 | 149.6 | 8.55 | 116.9 |
| C | 430 | 53.95 | 16.24 | 9.9 | 0.329 | 179.8 | 9.82 | 101.8 |
| D | 430 | 36.16 | 25.7 | 15.7 | 0.351 | 120.5 | 9.3 | 108 |
| B’ | 411.5 | 46.52 | 23.5 | 14.05 | 0.41 | 155 | 7.53 | 132.8 |
| C’ | 412.5 | 54.58 | 18.89 | 11.19 | 0.40 | 181.9 | 8 | 125 |
| D’ | 410.5 | 36.60 | 31.4 | 18.82 | 0.43 | 122 | 7.13 | 140.2 |

# CHAPTER 5
# CONCLUSION

This dissertation aims to propose design of flat band slow light on silicon in a photonic crystal waveguide with large delay bandwidth product and low GVD by shifting the positions of rows which are adjacent to the waveguiding region. The realization of on-chip slow light in silicon will open up new possibilities in the area because of the high refractive index contrast between Silicon slab (3.48) and air holes (1). A detailed study on band structure, group index, dispersion characteristics have been done in line-defect waveguide for two design approaches. Towards the applicability of proposed Structures in buffering we also calculated various parameters of buffering to analyses the structure more accurately.

A low-loss and flat dispersion line-defect photonic crystal waveguide is proposed with a simplified waveguide-design on silicon based on triangular lattice of two dimensional photonic crystals. We proposed two design approaches, in first approach, the lattice constant remains unchanged over all the designs – *A*, *B C* and *D*. Low dispersion and high group index bandwidth product for high group index values is obtained when we varied the positions of rows of holes. In the second set of approach, the lattice constant is varied in all designs – *A', B', C'* and *D'* and improvised NDBP over larger bandwidth is obtained. The idea of varying the lattice constant lies in the need of achieving slow light over same wavelength range where the dispersion is considered to be low. Band structure, group index and dispersion characteristics have been investigated for all proposed Structures. A delay-bandwidth product (NDBP) with acceptably small group velocity dispersion in photonic crystal waveguide is achieved. We proposed three Structures by shifting the first two rows of holes adjacent to the waveguide. Larger group index values of 36.16, 44.9 and 53.95 over flat bandwidth of 15.7, 13.66 and 9.9 nm along with NDBP values of 0.351, 0.38 and 0.329 are obtained. NDBP value is further improved by taking different lattice constant values for all three Structures and higher group indices 36.60, 46.52 and 54.58 over flat bandwidth of 18.82, 14.05 and 11.19 nm are reported. GVD parameter is also found to be low for all the Structures. The reported results can be useful in realizing flat band slow light in silicon with improved waveguiding characteristics. To

further test the practical applicability of our waveguide the buffering capacity is calculated which is found to be as high as 140 bits. Both the approaches are better from fabrication point of view as controlling the radius of holes at nano-metre scale brings fabrication challenges. The flat dispersive nature is one of the most vital features in line defect waveguides and it will open up new prospects for functional waveguide devices based on photonic crystals. Further the proposed design with static slow light can be modified to achieve dynamic slow light which eliminates all constraints in time, frequency and space. Slow light generated by devices with dynamically tuned parameters breaks the DBP constraint and can greatly reduce the slow down factor.

# REFERENCES


[1] J. D. Joannopoulos, R.D. Meade, J. N. Winn, “Photonic Crystals- Molding the Flow of Light”, Princeton Academic Press, Princeton, NJ, 1995.

[2] S. John, “Strong localization of photons in certain disordered dielectric super lattices”, *Physical Review Letters*, 58, 2486–2489, 1987.

[3] E. Yablonovich, “Inhibited spontaneous emission in solid-state physics and electronics”, *Physical Review Letters*, 58, 2059–2062, 1987.

[4] E. Yablonovitch, “Photonic band-gap structures,” *J. Opt. Soc. America*, vol. 10, pp. 283-295, 1993.

[5] T. F. Krauss, Richard M. De la rue, and Stuart brand, “Two-dimensional photonic-bandgap structures operating at near-infrared wavelengths,” *Nature* , vol. 383, pp. 699 - 702 , October ,1996

[6] R. Hamam, M. Ibanescu, S. Johnson, J. Joannopoulos, and M. Soljacic, "Broadband super-collimation in a hybrid photonic crystal structure," *Opt. Express*, vol. 17, pp. 8109-8118, 2009.

[7] Florencio García Santamaría, “Photonic crystals based on silica microspheres,” Ph.D. dissertation, Deptt. of Material Physics, Institute of Material Science of Madrid, Autonomous University of Madrid, October 2003.

[8] J. D. Joannopoulos, Pierre R. Villeneuve, and Shanhui Fan, “Photonic crystals: putting a new twist on light,” *Nature*, vol. 386, pp. 143- 149, March, 1997.

[9] http://www.rp-photonics.com/photonic_crystal_fibers.html

[10] S. Noda, and T. Baba, “Roadmap on Photonic Crystals”, Norwell, MA: Kluwer, 2003.

[11] O. Painter, R. K. Lee, A. Scherer, A. Yariv, J. D. O’Brien, P. D. Dapkus, and I. Kim, “Two-dimensional photonic band-gap defect mode laser,” *Science*, vol. 284, no. 5421, pp. 1819–1821, June 1999.

[12] F. Morichetti, Carlo Ferrari, Antonio Canciamilla, and Andrea Melloni, “The first decade of coupled resonator optical waveguides: bringing slow light to applications," *Laser & Photonics Reviews*, vol. 6, no. 1, pp. 74-96, 2012.

[13] A. Yariv, Y. Xu, R. Lee, and A. Scherer, “Coupled-resonator optical waveguide: a proposal and analysis," *Optics letters*, vol. 24, no. 11, pp. 711- 713, 1999.

[14] D. Ohnishi, K. Sakai, M. Imada, and S. Noda, “Continuous wave operation of surface emitting two-dimensional photonic crystal laser,” *Electron. Lett.*, vol. 39, no. 7, pp. 612–614, Apr. 2003.

[15] M. Yokoyama, and S. Noda, “Finite-difference time-domain simulation of two-dimensional photonic crystal surface-emitting laser having a square-lattice slab structure,” *IEICE Trans. Electron.*, vol. E87C, no. 3, pp. 386–392, 2004.

[16] K. Sakai, D. Ohnishi, T. Okano, T. Sakaguchi, and S. Noda, “Lasing bandedge identification for a surface-emitting photonic crystal laser,” *IEEE J.Sel. Areas Commun.*, vol. 23, no. 7, pp. 1335–1340, Jul. 2005.

[17] Fan Shanhui, M.F. Yanik, Wang Zheng, Sunil Sandhu, and M. L. Povinelli, "Advances in Theory of Photonic Crystals," *Journal of Lightwave Technology*, vol. 24, no.12, pp. 4493-4501, Dec. 2006.

[18] H. Kosaka, T. Kawashima, A. Tomita, M. Notomi, T. Tamamura, T. Sato, and S. Kawakami, “Superprism phenomena in photonic crystals,” *Phys. Rev. B, Condens. Matter*, vol. 58, no. 16, pp. R10096–R10099, Oct. 1998.

[19] M. Notomi, “Theory of light propagation in strongly modulated photonic crystals: Refraction like behavior in the vicinity of the photonic band gap,” *Phys. Rev. B, Condens. Matter*, vol. 62, no. 16, pp. 10696–10705, Oct. 2000.

[20] K. Orita, S. Tamura, T. Takizawa, T. Ueda, M. Yuri, S. Takigawa, and D. Ueda, “High-extraction-efficiency blue light-emitting diode using extended-pitch photonic crystal,” *Jpn. J. Appl. Phys.*, vol. 43, no. 8B, pp. 5809–5813, 2004.

[21] Toshihiko Baba, "Slow light in photonic crystals," *Nature photonics*, vol. 2, no. 8, pp. 465- 473, 2008.

[22] Erica Bennici, “Amorphous Silicon based Photonic Crystals,” Ph. D. Dissertation, Doctorate in Physics, School of Doctorate, Polytechnic University of Purin.

[23] Jagerska Jana, “Dispersion Properties of Photonic Crystals and Silicon Nanostructures Investigated by Fourier-Space imaging,” Ph.D. dissertation, Laboratory of Quantum optoelectronics, Institute of Physics and Condensed Matter, Ecole Polytechnique Federale de Lausanne.

[24] Phuong Chi Hoang, “Applications of Photonic Crystals in Communications Engineering and Optical imaging,” Ph.D. thesis, deptt. of electrical engg. and information tech., Technical University of kaiserslautem, 2009.

[25] Alexander Petrov, “Slow light photonic crystal line-defect waveguides,” Ph.D. dissertation, St. Petersburg, Technical University of Hamburg- Harburg, 2008.

[26] S. L. McCall, P. M. Platzman, R. Dalichaouch, D. Smith, and S. Schultz, “Microwave propagation in two-dimensional dielectric lattices”, *Phys. Rev. Lett*., vol. 67, pp. 2017-2020, 1991.

[27] R. D. Meade, K. D. Brommer, A. M. Rappe, and J. D. Joannopoulos, “Electromagnetic Bloch waves at the surface of a photonic crystal,” *Phys. Rev. B*, vol. 44, pp. 10961-10964, 1991.

[28] P. R. Villeneuve, S. Fan, J. D. Joannopoulos, “Microcavities in photonic crystals: mode symmetry, tunability and coupling efficency”, *Phys. Rev. B*, vol. 54, pp. 7837-7842, 1996.

[29] M. J. Steel, T. P. White, C. M. de Sterke, R. C. McPhedran, and L. C. Botten, “Symmetry and degeneracy in micro structured optical fibers,” *Optics Letters*, vol. 26, no. 8, pp. 488– 490, 2001.

[30] Clifford R. Pollock, and Tom Casson, “Fundamentals of Optoelectronics”, McGraw-Hill, New York, 1994.

[31] R. Hao, E. Cassan, X. Le Roux, D. Gao, V. Do Khanh, L. Vivien, D. Marris-Morini, and X. Zhang, "Improvement of delay-bandwidth product in photonic crystal slow-light waveguides," *Opt. Express*, vol.18, pp. 16309-16319, 2010.

[32] N. Moll., G. -L Bona, "Comparison of three-dimensional photonic crystal slab waveguides with two-dimensional photonic crystal waveguides: Efficient butt coupling into these photonic crystal waveguides," *Journal of Applied Physics*, vol. 93, no. 9, pp. 4986-4991, May 2003.

[33] C. J. Chang-Hasnain, and S. L. Chuang, "Slow and Fast Light in Semiconductor Quantum-Well and Quantum-Dot Devices," *Journal of Lightwave Technology* , vol. 24, no. 12, pp. 4642-4654, Dec. 2006.

[34] L. Frandsen, A. Lavrinenko, J. Fage-Pedersen, and P. Borel, "Photonic crystal waveguides with semi-slow light and tailored dispersion properties," *Opt. Express*, vol. 14, pp. 9444-9450, 2006.

[35] Fengnian Xia, Lidija Sekaric, and Yurii Vlasov, “Ultracompact optical buffers on a silicon chip,” *Nature Photonics*, vol. 1. pp. 65–71, 2006.

[36] L. O'Faolain, T. White, D. O'Brien, X. Yuan, M. Settle, and T. Krauss, "Dependence of extrinsic loss on group velocity in photonic crystal waveguides," *Opt. Express*, vol. 15, pp. 13129-13138, 2007.

[37] J. Li, T. White, L. O'Faolain, A. Gomez-Iglesias, and T. Krauss, "Systematic design of flat band slow light in photonic crystal waveguides," *Opt. Express*, vol. 16, pp. 6227-6232, 2008.

[38] T. F. Krauss, "Why do we need slow light?," *Nature photonics*, vol. 2, no. 8, pp. 448-450, 2008

[39] E. F. Burmeister, D. J. Blumenthal, and J.E. Bowers, "A comparison of optical buffering technologies," *Optical Switching and Networking*, vol. 5, no. 1, pp. 10-18, 2008.

[40] C. Monat, B. Corcoran, M. Ebnali-Heidari, C. Grillet, B. Eggleton, T. White, L. O'Faolain, and T. F. Krauss, "Slow light enhancement of nonlinear effects in silicon engineered photonic crystal waveguides," *Opt. Express*, vol. 17, pp. 2944-2953, 2009.

[41] A. Melloni, A. Canciamilla, C. Ferrari, F. Morichetti, L. O'Faolain, T.F. Krauss, R. De La Rue, A. Samarelli, M. Sorel, "Tunable Delay Lines in Silicon Photonics: Coupled Resonators and Photonic Crystals, a Comparison," *IEEE Photonics Journal*, vol. 2, no. 2, pp. 181-194, April 2010.

[42] H. Kurt, K. Üstün, and L. Ayas, "Study of different spectral regions and delay bandwidth relation in slow light photonic crystal waveguides," *Opt. Express*, vol. 18, pp. 26965-26977, 2010.

[43] J. Hou, H. Wu, D. Citrin, W. Mo, D. Gao, and Z. Zhou, "Wideband slow light in chirped slot photonic-crystal coupled waveguides," *Opt. Express*, vol. 18, pp. 10567-10580, 2010.

[44] Ran Hao, E. Cassan, H. Kurt, Jin Hou, X. Le roux, D. Marris-Morini, L. Vivien, Dingshan Gao, Zhiping Zhou, and Xinliang Zhang, "Novel Kind of Semi slow Light Photonic Crystal Waveguides With Large Delay-Bandwidth Product," *IEEE Photonics Technology Letters*, vol. 22, no. 11, pp. 844-846, June 1, 2010.

[45] M. Shinkawa, N. Ishikura, Y. Hama, K. Suzuki, and T. Baba, "Nonlinear enhancement in photonic crystal slow light waveguides fabricated using CMOS-compatible process," *Opt. Express* , vol. 19, pp. 22208-22218 , 2011.

[46] Yi Zhai, Huiping Tian, and Yuefeng Ji, "Slow Light Property Improvement and Optical Buffer Capability in Ring-Shape-Hole Photonic Crystal Waveguide," *Journal of Lightwave Technology*, vol. 29, no. 20, pp. 3083-3090, Oct.15, 2011.

[47] C. Caer, X. L. Roux, S. Serna, W. Zhang, L. Vivien, and E. Cassan , “Large group index bandwidth product empty core slow light photonic crystal waveguides for hybrid silicon photonics,” *Frontiers of Optoelectronics*, 2013.

[48] K. Kondo, M. Shinkawa, Y. Hamachi,Y. Saito, Y. Arita, and T. Baba, “Ultrafast Slow-Light Tuning Beyond the Carrier Lifetime Using Photonic Crystal Waveguides,” *Phys. Rev. Lett*., vol. 110, no. 5, pp. 053902, Jan. 2013.

[49] Jian Tang, Tao Wang, Xiaoming Li, Boyun Wang, Chuanbo Dong, Lei Gao, Bo Liu, Yu He, and Wei Yan, “Wideband and Low dispersion Slow light in Lattice-shifted photonic crystal waveguides,” *Journal of Lightwave Technology*, vol. 31, no. 19, Oct. 2013.

[50] J. Tang, T. Wang, X. Li, B. Liu, B. Wang, and Y. He, "Systematic design of wideband slow light in ellipse-hole photonic crystal waveguides," *J. Opt. Soc. Am. B*, vol. 31, pp. 1011-1017, 2014.

[51] S. Kubo, D. Mori, and T. Baba, "Low-group-velocity and low-dispersion slow light in photonic crystal waveguides," *Opt. Lett*., vol. 32, pp. 2981-2983, 2007.

[52] Y. Hamachi, S. Kubo, and T. Baba, "Slow light with low dispersion and nonlinear enhancement in a lattice-shifted photonic crystal waveguide", *Opt. Lett.*, vol. 34, pp. 1072-1074, 2009.